Extracellular traps and PAD4 released by macrophages induce citrullination and auto-antibody production in autoimmune arthritis

Mohey Eldin M El Shikh[a], Riham El Sayed[a], Alessandra Nerviani[a], Katriona Goldmann[a], Christopher Robert John[a], Rebecca Hands[a], Liliane Fossati-Jimack[a], Myles J. Lewis[a], and Costantino Pitzalis[a]*

[a] Centre for Experimental Medicine and Rheumatology, William Harvey Research Institute, Barts and The London School of Medicine and Dentistry, Queen Mary University of London, London EC1M 6BQ, UK

*** Corresponding Author**

Professor Costantino Pitzalis

Mailing Address

Centre for Experimental Medicine and Rheumatology William Harvey Research Institute

Barts and The London School of Medicine & Dentistry John Vane Science Centre

Charterhouse Square, London EC1M 6BQ, UK

Email: c.pitzalis@qmul.ac.uk

Abstract

The mechanisms underlying the transition of rheumatoid arthritis (RA) systemic autoimmunity to the joints remain largely unknown. Here, we demonstrate that macrophages in the secondary lymphoid organs (SLOs) and synovial ectopic lymphoid-like structures (ELSs) express peptidylarginine deiminase 4 (PAD4) in murine collagen induced arthritis (CIA) and synovial biopsies from RA patients. Moreover, peptidyl citrulline colocalized with macrophages in SLOs and ELSs, and depletion of macrophages in CIA decreased lymphoid tissue citrullination and serum anti-citrullinated protein/peptide antibody (ACPA) levels. Furthermore, PAD was released from activated murine and RA synovial tissue and fluid (SF) macrophages which functionally deiminated extracellular proteins/peptides *in vitro*. Additionally, activated murine and SF macrophages displayed macrophage extracellular trap formation (METosis) and release of intracellular citrullinated histones. Moreover, presentation of citrullinated proteins induced ACPA production *in vitro*. Thus, lymphoid tissue macrophages contribute to self-antigen citrullination and ACPA production, indicating that their selective targeting would potentially ameliorate citrullination-dependent autoimmune disorders.

Keywords: Macrophage Extracellular Traps, Lymphoid Tissues, Peptidyl Arginine Deiminase, Rheumatoid Arthritis, Citrullination, Anti-Citrullinated Protein/Peptide Antibody.

1. Introduction

Citrullination of various human proteins during the pre-clinical phase of rheumatoid arthritis (RA) is critical to breach of tolerance to self-antigens whose immune recognition may cross-react with joint antigens to initiate the disease [1, 2]. The pre-clinical phase of RA may last years during which humoral and cellular factors, including macrophages [3] contribute to the generation of citrullinated antigens and induction of anti-citrullinated protein/peptide antibodies (ACPA) in secondary lymphoid organs (SLOs). In fact, compelling evidences supporting the role of SLOs in the generation and perpetuation of arthritogenic autoimmunity have emerged. In parallel with the appearance of serum auto-antibodies (-Abs), antigen-specific B and plasma cells localize within germinal centres (GCs) and medullary cords of peripheral reactive lymph nodes (LNs), and IgM rheumatoid factor (RF) is detectable in the LNs of 100% of seropositive patients but not in normal controls [4, 5]. Moreover, the autoimmune response in experimental arthritis was shown to start specifically in the LNs draining target joints, spreading thereafter to other lymphoid stations including the spleen [6]. However, the mechanism(s) mediating selective localisation of the disease to the joints, and the cells contributing to synovial membrane homing have not been fully decoded. As the disease progresses, ectopic lymphoid-like structures (ELS) with active GCs develop in a large proportion of RA synovia [7-9] and the joints of mice with collagen-induced arthritis (CIA) providing plausible explanation for systemic-to-local transmission of the disease [10].

Citrullination corresponds to the conversion of arginine to citrulline by peptidylarginine deiminases (PADs). Five highly related calcium-dependent PADs have been described, and PAD4 is primarily expressed in the cells of the immune system and localizes to the cytoplasm and the nucleus [11, 12]. PAD2 and PAD4 are expressed in the synovial tissue of patients with RA and other arthritides, and inflammatory cells are a major source of PADs although PAD4 also comes from hyperplastic synoviocytes [13]. A pathogenic role of PAD4 in autoimmune

arthritis has been illustrated in studies showing that PAD4 knockout mice develop less severe arthritis [14] and that global inhibition of PAD4 ameliorates CIA [15].

Systemic and local ACPA production has been related to SLOs and chronically inflamed synovia with ELS respectively [16]. At the synovial level, recent studies from out laboratory illustrated the production of ACPA recognising citrullinated histones contained in neutrophil extracellular traps (NETs)[17]. However, while neutrophils are scarce in RA synovial membranes, resident macrophages are abundant, they are topographically in proximity of ELS and can function as antigen presenting cells. This prompted us to hypothesise that macrophages associated with SLO and ELS express PAD and contribute to antigen citrullination and drive autoimmunity in arthritis.

Using SLOs from CIA mice and synovial biopsies with ELSs from RA patients, we provide evidences that macrophages secrete functional PAD4 which deiminates extracellular antigens, colocalize with lymphoid tissue peptidyl citrulline and release citrullinated histones by macrophage extra cellular trap formation (METosis). We also show that presentation of citrullinated proteins by follicular dendritic cells (FDCs) to B cells induces ACPA production in germinal centre reactions (GCRs) in a T cell dependent manner. Thus, our results support a novel role for macrophages in citrullinating proteins and driving autoantibody production via an FDC/T-cell dependent pathway both in SLO and ELS in the rheumatoid synovia, providing a mechanism for establishing and maintaining the disease in the joint.

2. Materials and Methods

2.1. Mice and collagen induced arthritis (CIA)

DBA/1 mice (males, 8-12 weeks of age) were purchased from Harlan Envigo, UK, and housed in the Biological Service Unit (BSU) at William Harvey Institute – Charterhouse Square – London – UK. To induce CIA, mice were sensitized to bovine collagen type II (MDBioscience, 804001) in Freund's complete adjuvant, and synchronized with a boost of collagen in incomplete adjuvant on day 21. Mice were lightly anesthetized with isoflurane. The base of the tail was shaved and 100 µl collagen II/FCA emulsion (0.1 mg *M.tb.,* H37RA, Difco, 231141/100 µL Freund's incomplete adjuvant, Sigma F5506; Final concentration 200 µg collagen II/100 µL FIA) was injected intradermally to the left-hand side of this site. 21 days after initial sensitization, collagen II was dissolved in acetic acid as above, emulsified in Freund's incomplete adjuvant and 100 µL (200 µg collagen II) injected into the base of the tail on the right-hand side of the tail base. Mice were individually marked and assessed by blind observation three times a week for the development of arthritis and the clinical arthritis scores were recorded. Every inflamed main digit scored one, inflammation of the front paw scored one, inflammation of the hind paw scored one, and involvement of the ankle scored one. Thus, a maximal score for each animal was 22, and results were expressed as the total arthritis score of the group (6-8 mice / group). All experimental procedures were approved by the UK Home Office (project license PIL 70/23296).

2.2. RA synovial tissues and histological grading

Synovial tissues were obtained by ultrasound-guided synovial biopsy from DMARD-naïve patients with early (<12 months) RA (n=99), enrolled in the Pathobiology of Early Arthritis Cohort (PEAC) cohort (http://www.peac-mrc.mds.qmul.ac.uk) of the Centre for Experimental Medicine and Rheumatology of Queen Mary University of London as previously described

[18]. All patients fulfilled the 2010 EULAR criteria for RA [19]. Patients had clinically defined synovitis but duration of symptoms of less than 12 months and were all naïve to DMARD and steroid therapy. Upon enrollment, patients underwent ultrasound-guided synovial biopsy of a clinically active joint [18]. All procedures were performed following written informed consent and were approved by the hospital's ethics committee (REC 05/Q0703/198). Synovitis was semi-quantitatively assessed (0-9) according to a previously validated score (Krenn) [20]. Sequentially cut sections were stained with anti CD20cy (L26), CD3 (F7.2.38), CD68 (KP1), and CD138 (MI15) all from DAKO and each slide underwent SQ scoring (0-4), as previously reported [7]. Synovial pathotypes were defined as i) Lymphoid (L) CD20≥2 and/or CD138>2; ii) Myeloid (M) CD68SL≥2, CD20≤1 and/or CD3≥1, CD138≤2; and iii) Fibroid (F) CD68SL<2 and CD3, CD20, CD138<1

2.3. Immunohistochemistry and confocal imaging

SLOs (spleens and LNs) from CIA mice and synovial tissues with ELSs from RA patients were embedded in O.C.T (Sakura) and 10 μm cryo-sections were cut and fixed in ice cold acetone. The slides were rehydrated/Blocked with 2% horse serum (Jackson

→ ImmunoResearch, 008-000-121) in PBS at room temperature in a humidified chamber, then incubated at room temperature with primary Abs for 2 hrs followed by 3x wash in PBS then incubation with secondary Abs for 1 hr. After incubation with the secondary Abs, the slides were washed in PBS 3 times, dried and mounted with Vectashield Antifade Mounting Medium (Vector Laboratories), cover-slipped, and examined with a Leica TCS SP2 AOBS confocal laser-scanning microscope. Three lasers (488, 543, and 633 nm) were used and far red emission is shown as pseudo-colour. Parameters were adjusted to scan at 1024 x 1024-pixel density and 8-bit pixel depth. Emissions were recorded in three separate channels, and digital images were captured and processed with Leica Confocal Software LCS Lite. The Abs

used in this study are listed in the table 1 and their concentrations ranged between 5 and 10 μg/ml.

2.4. Measurement of tissue citrulline

The citrulline content in mice spleens was measured using the quantitative sandwich ELISA Mouse Citrulline (CIT) ELISA kit (Cat#MBS027373, MyBioSource, San Diego, CA) according to the manufacture instructions and data was expressed as the optical density (O.D.) read at 450 nm.

2.5. Macrophage depletion

Macrophages were depleted in DBA/1 mice by i.p injection of 250 μg / mouse F4/80 mAb for three successive days before CIA induction. The F4/80 ATCC® HB-198™ hybridoma was used for the generation of sufficient amounts of the mAb F4/80 that was purified from the culture supernatants on protein G columns in the protein purification facility at Queen Mary University of London. The efficacy of depletion was assessed before CIA induction using multicolour flow cytometry of single cell suspensions prepared from the spleens and LNs.

→ After Fc blockade with TruStainFcX (Biolegend, 101320), a panel of CD19 PE (Biolegend, 115508), CD3 AF488 (Biolegend, 100321), CD11b BV605 (Biolegend, , 101257) and F4/80 PE-Cy7 (Biolegend, 123114) was used and the plots were gated on the non B / non T cells. The % of $F4/80^+$ cells in treated and untreated mice groups was calculated.

2.6. Murine FDC, B cell, and T cell isolation

FDCs were isolated by positive selection from normal DBA/1 mice spleens and LNs as recently described [21]. Briefly, single cell suspensions were prepared from the tissues then

→ sequentially incubated with FDC-specific Ab (FDC-M1, BD Biosciences, 551320) for 45 min, 1 μg of biotinylated anti-rat κ L chain (BD Biosciences, 553028) for 45 min, and 20 μl of anti-biotin microbeads (Miltenyi Biotec, 130-090-485) for 15–20 min on ice. The cells were

→ layered on a MACS LS column (Miltenyi Biotec, 130-041-306) and washed with 10 ml of ice-cold MACS buffer. The column was removed from the VarioMACS, and the bound FDCs were released with 5 ml of MACS buffer. $B220^+$ B cells were isolated from CIA mice using CD45R (B220) MicroBeads from Miltenyi Biotec (130-049-501), and T cells were purified using the Pan T Cell Isolation Kit II, mouse (Miltenyi Biotec, 130-095-130).

2.7. Macrophage isolation and in vitro activation

Murine macrophages were purified using EasySep Mouse CD11b Positive Selection Kit II
→ (STEMCELL Technologies, 18770). Macrophages were tagged with CD11b Abs and magnetic particles, then isolated using an EasySep magnet. A stock solution of 1mg/ml LPS
→ (InvivoGen, UK, tlrl-eklps) was prepared using endotoxin-free water and $1x10^6$ purified macrophages were stimulated with 10, 100, and 1000 ng/ml LPS in 400 ul DMEM for 4 hours in 8-well culture slides. Unstimulated and PMA -stimulated (1 μg/ml) cells were used as
→ negative and positive controls respectively. PMA was burchased from SigmaAldrich (P8139). Culture supernatants were collected and assessed for PAD release by ELISA, and attached macrophages were stained with nuclear stain and anti-citrullinated histones to visualize METosis by confocal microscopy.

2.8. Activation and visualization of METosis in synovial fluid (SF) macrophages

SF samples were obtained from inflamed knees of $ACPA^+$ patients in sterile Na Heparin vacutainers and the cells were collected by centrifugation at 2,000 rpm for 10 minutes. PMNLs and mononuclear cells were isolated by double density gradient centrifugation using
→ Histopaque 1119 (SigmaAldrich, 11191) and Histopaque 1077 (SigmaAldrich, 1077). The mononuclear cells were harvested, counted and macrophages were enriched by attachment then stimulated with LPS as described in the murine macrophages. Unstimulated human tonsillar macrophages were included as a control, culture supernatants were collected after 24

hrs, and PAD activity was assessed in the supernatants on fibrinogen coated ELISA plates. Slide preparations of SF macrophages were Giemsa stained and visualized by light microscopy. Nuclei, PAD4 and citrullinated histones were also stained and assessed by confocal microscopy.

2.9. Synovial organ cultures

RA synovial biopsies were cut into small homogenous pieces (i.e. 20-40mg) avoiding fat and connective tissue. The synovial pieces were gently transferred into cell culture inserts (Millicell, PIHA01250) mounted in 24-well plates containing 600 ul RPMI with 10% FCS. A drop of medium was added on top of the tissues and the plates were incubated for 24h at 37°C. After 24 hrs, 300 µl from each well were collected and replaced with 300µl medium for further 24 hrs then culture supernatants were collected and synovial tissue lysates were prepared.

2.10. *In situ* citrullination of fibrinogen

The ability of the released PAD in the culture supernatants of RA SF macrophages and organ cultures to citrullinate extracellular antigens was assessed by in situ citrullination of native
→ human fibrinogen (SigmaAldrich, F3879). To generate a standard curve, human fibrinogen
→ was first citrullinated using rabbit skeletal muscle PAD (SigmaAldrich, P1584) (7 U/mg fibrinogen) and used for ELISA coating starting with 0.5 µg/mL with 1:2 serial dilution. Samples were incubated on native fibrinogen-coated wells (250 ng/ml) for 4 hours at $37^{O}C$ and $CaCl^{+2}$ in the reaction mixture was adjusted to 10mM. Generation of citrulluinated fibrinogen due to PAD activity was then assessed using human anti-citrullinated fibrinogen mAb (ModiQuest, clone 1F11 CAT No. MQR 2.101-100) that specifically binds deiminated but not native fibrinogen. The human mAb was detected using HRP-conjugated goat anti
→ human IgG secondary (Thermofisher Scientific, 62-8420) HRP was developed using TBM

→ (Vectorlabs, SK-4400), and ODs at 450 nm were read using multiwall plate reader (BMG LABTECH, UK) and MARS data analysis software.

2.11. PAD activity ELISA assay

PAD activity in the undiluted culture supernatants of activated murine macrophages was assessed using Ab Based Assay for PAD activity (ABAP) (ModiQUEST, MQ17.101-96) following the manufacturer instructions. Principally, after incubation of the culture supernatants on plates pre-coated with arginine-containing peptides, an HRP-labelled monoclonal mAb is used to detect deiminated arginine (citrulline) and the ODs measured at 450 nm after development of the TBM substrate are calculated.

2.12. Immune complex (IC) preparation and in vitro GCRs

CIA sera react with citrullinated but not native human fibrinogen [22]. Citrullinated fibrinogen ICs were generated by incubating 100 ng citrullinated human fibrinogen with 100 ul serum taken from CIA mice with anti-cyclic citrullinated peptides (CCP) > 50 U/ml for 1 h at 37°C. The ICs were loaded on FDCs for 1 hr at 37^{O}C then the cells were washed in PBS and retention was confirmed by IF using rabbit anti-human fibrinogen Ab followed by rhodamine-conjugated anti rabbit secondary. FDCs were then co-cultured with B and T cells purified from the CIA spleens where 1x10^{6} B cells/culture were used at a ratio of 1 FDC : 2 B cells : 1 T cell. In vitro cultures were maintained for 5 days, then undiluted culture supernatants were assessed for anti-CCP IgG production using ELISA.

2.13. In vitro generation of Tingible Body Macrophages (TBM)

Purified murine B cells were labelled with CSFE using the CellTrace™ CFSE Cell Proliferation Kit (ThermoFisher, C34554) then incubated with anti-mouse CD95 (Fas) Ab
→ (Biolegend, 152803)(0.25/ μg/10^{6} cells) at 37°C for 3 hours to induce B cell apoptosis. Apoptotic B cells were then incubated with splenic macrophages enriched by attachment for 3

hours to allow uptake and TBM generation. TBMs were stimulated with 10 ng/ml LPS for 4 hours in slide cultures then stained with anti CD68 and nuclear stain and METosis of TBMs was assessed by confocal microscopy.

2.14. Measurement of anti-CCP levels

Axis-Shield anti-CCP ELISA kit (Axis-Shield Diagnostics Ltd, FCCP600) was used according to the manufacturer instructions with modifications to assess mouse anti-CCPs. The secondary anti human Ab provided in the kit was replaced with an anti-mouse HRP conjugated secondary (AffiniPure Goat Anti-Mouse IgG (H+L) (Jackson ImmunoResearch 115-035-003 diluted 1:5000). Sera were used at 1:10 dilution; and culture supernatants were assessed undiluted with data calculated after subtraction of potential backgrounds due to Abs
→ in the ICs. The cut-off for the sera followed a previous report applying a similar protocol and using sera from *Rag1*$^{-/-}$ and unimmunized DBA/1 mice [22]. The cut-off for culture supernatants was calculated as 3 standard deviations above the mean value of unstimulated B cell cultures from unimmunized DBA/1 mice.

Preparation of tissue and cell lysates and immunoblotting

Murine tissue and cell lysates from the skin, spleens, LNs, and purified macrophages were prepared by homogenization in Ripa buffer and 1% protease inhibitor cocktail. Protein concentrations were determined using BCA Protein assay and 25 μg protein / sample were separated by SDS PAGE. Recombinant mouse PAD4 and GAPDH were used as controls, and MW markers were included. Proteins separated by SDS-PAGE were imaged by UV then transferred to nitrocellulose membranes and the immunoblots were incubated with mouse anti-PAD4 (Santa Cruz, sc-365369) diluted 1:500 followed by goat anti-mouse IgG-HRP
→ (Santa Cruz, sc-2005) at 1:2000 dilution. Clarity Max Western ECL Substrates (Bio-rad,

1705061) was used for detection and membranes were exposed to Amersham films that were developed and fixed.

2.15. RNA-Seq analysis

CD68 and PADI4 expression were analysed using RNA-Seq data generated from RA synovial tissue and matched blood samples enrolled in the PEAC cohort. Transcript abundance was derived from FASTQ files over GENCODE v24/GRCh38 transcripts using Kallisto v0.43.0. Transcript abundances and average transcript lengths were imported into R using Bioconductor package tximport 1.4.0 and summarised over NCBI RefSeq transcript isoforms. Imported abundances were normalised in R, including a correction for average transcript length and incorporating batch, sex, and pathotype as model covariates, using DESeq2 1.14.1. Transcript abundances underwent regularised log expression (RLE) transformation and depicted on the Y axis whereas the synovial pathotypes were shown on the X axis. Differential expression analysis based on negative binomial distribution using regression models of normalised count data was performed using DESeq2 and a likelihood ratio test to compare variation between pathotype groups in the synovium followed by pairwise comparisons between Lymphoid, Myeloid and Fibroid groups. P values were converted to Q values based on Benjamini-Hochberg false discovery rate (FDR), using FDR cut-off set at $Q<0.05$ to define differentially expressed genes.

2.16. Mander's colocalization coefficient

In situ correlation of CD68, peptidyl citrulline, and PAD4 was analyzed using the Mander's (R) overlap coefficient plugin in Image J. Before running the algorithm, backgrounds were subtracted, and thresholds were automatically assigned. Correlation plots were generated and coefficients calculated. Mander's R colocalization ranges between 0 = no localization, and 1 = maximum colocalization.

2.17. Statistical analysis

Significant differences were calculated with GraphPad using Student's T test and p values of < 0.05 were considered statistically significant.

3. Results

3.1. PAD4 is expressed in the secondary lymphoid tissues of CIA mice and colocalizes with CD68^{+} macrophages

In RA, ACPA production precedes the onset of clinical arthritis indicating a role of extra articular sites, peripheral and lymphoid, in autoantigen citrullination and autoAb production. Here, we sought to see if ACPA production similarly precedes arthritis in CIA mice; and evaluate the expression and source of the citrullination enzyme PAD4 at the peripheral site of antigen challenge, the skin, and the secondary lymphoid tissues draining this site.

First, we induced CIA in male DBA/1 mice and assessed the total arthritis score and the anti-CCP levels in the sera of these mice. Figure 1-A demonstrates that by day 21 anti-CCP Abs were detectable in the sera of CIA mice but not in unimmunized controls. While anti-CCP autoAbs were measurable in the sera of CIA mice at day 21, arthritis was not clinically detectable, and the total arthritis score was comparable with unimmunized controls (Figure 1-
→ B) indicating that anti-CCP Abs precedes clinical arthritis in CIA. The anti CCP levels were further measured on day 28 and at a terminal bleed on day 42 attaining levels of 30$\pm$9 (SEM) and 41$\pm$12 (SEM) respectively. Using unpaired 2-tailed student T test, the serum levels of anti CCP were significantly higher on day 42 ($p = 0.047$) but not on day 28 ($p = 0.25$) when compared to day 21.

Induction of anti-CCP Abs requires citrullination of auto-antigens, and consequently we sought to determine whether the citrullination enzyme PAD4 is expressed at the site of antigen entry, the skin, and / or the inguinal and popliteal LNs draining the skin of the base of the tail of CIA mice. Western blotting (WB) of the skin and LN lysates from 3 different mice (Figure 1-C) showed that PAD4 immunosignal was detectable at the expected MW (~67 Kd) in the draining LNs but not in the skin lysates indicating that SLOs are sites of PAD4

expression where citrullinated proteins and peptides could be generated and presented. Furthermore, PAD4 was also expressed in other SLOs, the spleens, of CIA mice, as indicted by WB (Figure 1-D).

Neutrophil-PAD4 has been associated with the pathogenesis of autoimmune arthritis, however, neutrophils are not abundant in SLOs, prompting our investigation of the cellular source of PAD4 in these tissues. Our preliminary studies indicated that PAD4 is distributed in macrophage-rich areas of SLOs, suggestive of a macrophage source of this enzyme. To test this, we performed confocal imaging of immuno-labelled cryo-sections of CIA spleens and DLNs as shown in Figure 1-E, and 1-F. Dual and triple overlays of PAD4, CD68, and CD11c staining indicated that PAD4 maximally co-localizes with $CD68^+$ macrophages in the spleen and LNs with less overlap with the dentritic cell marker CD11c. In fact, PAD4 followed the regional distribution of CD68 in the subcapsular sinus, the paracortical, and the medullary regions of the DLNs with relatively less expression in the B cell follicles in the cortex (Figure 1-F). Furthermore, high magnification imaging of the DLN medullary regions (Figure 1-G) resolved intracellular expression of PAD4 in $CD68^+$ macrophages. Moreover, PAD4 was detectable in the GC induced in the DLNs of the CIA mice and colocalized with $CD68^+$ tingible body macrophages (TBMs) containing $GL7^+$ fragments of GC B cells (Figure 1 H-J). To further confirm that SLT macrophages produce PAD4, lysates of CD11b-purified macrophages from the spleen and LNs were analysed by WB and the PAD4 immunosignal was detectable at the expected MW (~67 Kd) in lysates prepared from 3 different CIA mice (Figure 1-K). Overall, this supports that macrophages express PAD4 in SLOs of CIA mice where citrullinated proteins and peptides can be presented to induce ACPA production.

3.2. Citrullinated proteins/peptides colocalize with $CD68^+$ macrophages in the draining LNs and spleens; and macrophage depletion decreases lymphoid tissue citrulline and serum ACPA levels in CIA mice

Having established the expression of PAD4 by macrophages in CIA SLOs, we then proceeded to investigate the distribution of citrullinated proteins/peptides in relation to the macrophages' CD68 and assess the impact of macrophage depletion on SLOs citrulline content and serum anti-CCP levels. Our initial attempts (not shown) to label citrullinated proteins/peptides in SLOs were associated with high backgrounds due to Ab binding to both free and peptidyl citrulline. Since free citrulline is a member of the citric acid cycle and its metabolism is not regulated by peptidyl arginine deiminases (PADs) or associated with the pathogenesis of autoimmune arthritis, we used a mAb (anti-peptidyl citrulline, clone F95) that specifically binds peptidyl- and protein-bound citrulline but not the free form of citrulline. Figure 2-A illustrates the distribution of citrullinated peptides/proteins in the DLNs of CIA mice with overlays showing colocalization with CD68+ macrophages (Figure 2A i-ii). In the LN cortex (Figure 2A iii), peptidyl citrulline colocalized with the subcapsular sinus macrophages and displayed a dendritic pattern in the B cell follicles suggestive of retention on FDCs. This was later confirmed by colocalization with FDC-CD21 and the GC B cell marker GL7 (Figure 5). Similarly, citrullinated peptides/proteins colocalized with $CD68^{+}$ macrophages in the spleen (Figure 2B i) and showed intrafollicular dendritic pattern suggestive of FDC association.

The presence of citrullinated peptides/proteins in association with SLOs macrophages prompted us to investigate the impact of macrophage depletion on the citrulline content of these organs and if decreased citrulline is associated with lower serum anti-CCP levels. To test this, macrophages were depleted in DBA/1 mice by i.p. administration of the mAb F4/80 for three successive days before induction of CIA and effective depletion was assessed by flow cytometry. As expected, F4/80 treatment reduced the $F4/80^{+}$ cells in the different subsets of splenic macrophages ($F4/80^{+}$ / $CD11b^{-}$, $F4/80^{+}$ / $CD11b^{lo}$, and F4/80+ / $CD11b^{hi}$) compared to PBS treated controls (Figure 2C and D) with less effect on $F4/80^{-}$ macrophages. Moreover,

macrophage depletion by F4/80 was associated with significant reduction ($p < 0.05$) in the citrulline content of the CIA spleens 3 and 4 weeks after CIA induction (Figure 2E); which correlated with significant inhibition in serum anti-CCP levels ($p < 0.05$) compared to mAb-untreated mice (Figure 2F). Macrophages repopulated lymphoid tissues in macrophage-depleted mice with comparable ratios in F4/80-treated and controls 3 weeks after collagen II administration as previously reported [23]. Collectively, this suggests that macrophages contribute to the generation of citrullinated proteins in SLOs and their depletion reduces the tissue citrulline content and the serum anti-CCP levels.

3.3. Activated macrophages release PAD4 and exhibit extracellular trap formation (METosis)

The preceding data suggest that macrophages contribute to the level of citrullinated antigens in SLOs which in turn influences the serum anti-CCP levels. Thus, we next sought to reveal potential mechanisms that may underly this contribution. Full differentiation of B cells into anti-CCP-producing plasma cells requires co-signals from antigen-specific T cells which can be stimulated by macrophages as professional antigen presenting cells. However, T cell help is not the sole requirement for B cell activation, and effective engagement of the BCR with antigens in the extracellular space is essential for cognate recognition and antigen-specific B cell responses. Both extracellular (e.g. citrullinated fibrinogen), and intracellular (e.g. citrullinated histones) antigens are targeted by ACPAs in autoimmune arthritis; and we reasoned that macrophage activation contributes to the availability of both targets by PAD4 release and macrophage extracellular trap formation (METosis) respectively. A vast array of molecules can activate macrophages in the context of autoimmune arthritis, including but not limited to proinflammatory cytokines, TLR ligands, and ICs; and we used LPS as a classic macrophage activator. To test citrullination of extracellular antigens by released macrophage PAD4, we used commercial ELISA plates coated with arginine-containing peptides and detected conversion of arginine into

citrulline using specific anti-citrulline Ab. Figure 3A indicates that unstimulated murine splenic macrophages release PAD4 at baseline, and this release can be significantly induced by PMA (positive control) and different concentrations of LPS. To further investigate if activated macrophages can also contribute to the provision of citrullinated intracellular targets via METosis, murine splenic macrophages were stimulated with PMA and LPS and stained with nuclear and citrullinated histone stains. As shown in figure 2B, activated macrophages released intracellular citrullinated histones that were detectable in the extracellular space but not in unstimulated controls (Figure 3B). TBMs are unique subset of lymphoid tissue macrophages that promote peripheral tolerance by eliminating apoptotic B cells from the GCs. However, this critical role can be reversed if macrophage activation also induces METosis in TBMs when not only macrophage citrullinated proteins will be released in the vicinity of the GCs, but also their cargo of apoptotic B cell fragments will be made available to the hypermutating BCRs. To this end, we generated TBMs in vitro using CSFE-labelled apoptotic B cells and stimulated them with LPS and visualized the cells with confocal microscopy. As shown in figure 3C, apoptotic B cell fragments were released from TBMs in association with the DNA extra cellular traps. Altogether, these data suggest that activated macrophages contribute to the availability of extracellular and intracellular citrullinated antigens by releasing PAD and METosis respectively.

3.4. Anti-CCP Ab production is T cell dependent

The mere availability of citrullinated antigens would not effectively induce B cell activation, plasma cell differentiation, and anti-CCP production. GCs are the hotspots in lymphoid tissues where FDCs and primed Tfh cells provide antigenic and non-antigenic signals that efficiently activate B cells and induce class switching and high affinity Ab production. While FDCs present antigens to B cells as ICs in the GCs of the LN cortex, T cell priming mainly occurs in the deep cortical units (paracortex) which, following activation, migrate to the GCs, where they provide cognate help and ICOS/CD40L-mediated B cell co-stimulation. Together

with FDC-derived co-signals, Tfh cells induce CSR, SHM, affinity maturation and memory B cell generation. Here we asked if (1) peptidyl citrulline colocalizes with macrophages interacting with T cells in the paracortex, and FDCs interacting with GC B cells in the cortex; (2) activation of B cells with citrullinated fibrinogen loaded-FDCs requires T cells for anti-CCP IgG production in *in vitro* GCRs. To answer these questions, we first used confocal imaging of the DLNs of CIA mice to delineate the association of peptidyl citrulline with FDCs and macrophages. Figure 4A illustrates the colocalization of peptidyl citrulline with $CD68^+$ macrophages and $CD3^+$ T cells in the paracortex where T cell priming occurs, while figure 4B shows peptidyl citrulline retention on the $CD21^+$ FDC reticula where B cell activation by FDC-ICs is induced. In addition, well-developed GCs supported by peptidyl citrulline-retaining FDCs and $ICOS^+$ Tfh cells (Figure 4C), were detectable in association with Blimp-1^+ plasma cells (Figure 4D) in the secondary B cell follicles situated in the cortices of the draining LNs. We have previously demonstrated a novel T cell-independent pathway of B cell activation by multimerized antigens on FDCs [24, 25] where extensive crosslinking of the BCRs by FcγRIIB-retained antigens in the presence of FDC-derived BAFF and C4bBP induced robust GCRs and antigen-specific Ab response. So, we sought to determine if a similar T independent pathway could mediate B cell activation and anti CCP autoAb production in autoimmune arthritis. To test this, we purified FDCs from normal DBA/1 mice spleens and loaded them with citrullinated fibrinogen ICs (Figure 4E), then, we set up *in vitro* GCRs (Figure 4F) using IC-loaded FDCs with B and T cells purified from CIA spleens where the presence of citrullinated fibrinogen specific CD4 T cells has been previously substantiated [26]. Cultures were maintained for 5 days then anti-CCP IgG was measured by ELISA. As shown in figure 4G, anti-CCP IgG was induced only in the presence of T cells and citrullinated fibrinogen on FDCs but not in antigen- or T cell-deficient cultures. Collectively, the synergistic effect of Tfh-mediated B cell co-stimulation and the presentation

of citrullinated antigens by FDCs to B cells during the GCR are critical for induction of anti-CCP IgG autoAbs.

3.5. Tissue macrophages expressing PAD4 colocalize with peptidyl citrulline, and correlate with ELSs in RA synovium

We next investigated whether results obtained in the murine CIA SLOs were operational in in RA synovial tissues. First, we assessed PAD4 expression and peptidyl citrulline distribution in the synovial membranes using IHC. Figure 5A indicates that PAD4 colocalizes with $CD68^+$ macrophages in the inflamed synovia, however, its distribution is not restricted to macrophages. In fact, a strong PAD4 signal with serpentine pattern, suggestive of a vascular association, is detectable in the synovial tissues distinguishable from the CD68 macrophage marker. In addition, peptidyl citrulline colocalized with intimal and subintimal $CD68^+$ macrophages in the RA synovium (Figure 5B). Furthermore, PAD4 expressing $CD68^+$ macrophages were present within follicular structures mirroring TBMs of the GCs (Figure 5C). To compare the relative distribution of peptidyl citrulline in relation to macrophages, T cells, FDCs, and B cells, we used adjacent sections from RA synovia with ELS and scanned them for different cellular components. As observed in the CIA SLOs, peptidyl citrulline colocalized with $CD68^+$ macrophages interacting with $CD3^+$ T cells (Figure 5D), retained on $CD21^+$ FDCs (Figure 5E) in association with well-formed ELS ($CD20^{hi}$, $CD3^+$; figure 5F). Moreover, the plasma cell transcription factor Blimp-1 was detectable in these ELSs as shown in figure 5G. The association of $CD68^+$ macrophages with the cellular architecture of ELSs in RA synovia was further confirmed by RNA-Seq expression analysis. Figure 5H shows that CD68 expression significantly correlate with the lymphoid and myeloid pathotypes compared to the fibroid synovial pathotypes (Lymphoid v Myeloid adjusted *p* 1.1e-01; Myeloid v Fibroid adjusted *p* 6.5e-02; Lymphoid v Fibroid adjusted *p* 3.6e-05). In addition, CD68 expression is significantly higher in the lymphoid pathotype and strongly correlates with the

histological scoring of the T, B, and plasma cell markers CD3, CD20, and CD138 respectively. Moreover, CD68 significantly correlates with the genes encoding CD3epsilon (T cell, also CD3gamma and CD3delta – data not shown), MS4A1 (B cell, CD20), CR2 (FDC, CD21), and PRDM1 (plasma cell, Blimp-1) (Figure 5I). We also calculated the co-distribution of CD68, peptidyl citrulline, and PAD4 in the RA synovium using Mander's colocalization algorithm where 0 indicates no colocalization and 1 indicates maximum colocalization. Mander's correlation coefficients were 0.7+ 0.4, 0.76+0.6, 0.75+0.5 for CD68/peptidyl citrulline, PAD4/peptidyl citrulline, and CD68/PAD4 co-distribution respectively (Figure 5J i-vi]. While intracellular PAD4 colocalized with the macrophage marker CD68 (Figure 5J vii white box), and extracellular PAD4 (Figure 5J vii dashed white box) was seen in proximity to macrophages, again (as seen in Figure 5A), a distinct signature of PAD4, potentially associated with vessel walls but not with macrophages, was evident in the RA membranes (Figure 5J vii double white box). Thus, although SLOs are developmentally dictated while ELSs are inducible by inflammation, the expression of PAD4 by macrophages, the retention of peptidyl citrulline on FDCs, and the interaction between the different cellular components display similar mechanisms.

3.6. RA synovial fluid (SF) macrophages and synovial organ cultures release PAD and citrullinated histones and display METosis

Given some similarities between SLOs and ELSs regarding PAD4 expression and peptidyl citrulline association with macrophages, we speculated that similar mechanisms of PAD release and METosis by RA macrophages could contribute to the provision of citrullinated extracellular and intracellular antigens respectively. To this end we separated macrophages from freshly aspirated SF using Ficoll followed by attachment then stimulation with LPS. Human tonsillar macrophages enriched by attachment were used as a control. In addition, ELS^+ RA synovial tissue organ cultures (whole tissue – without macrophage purification)

were also tested. As illustrated in figure 6A-i, PAD activity was significantly higher in freshly isolated SF macrophages culture supernatants compared to control tonsillar macrophages, and stimulation with LPS did not promote further activation. In addition, PAD was secreted in the culture supernatants of RA synovial organ cultures (figure 6B) as detected using *in situ* citrullination of native fibrinogen as a read out (figure 6B-i). We also stained freshly isolated SF macrophages to assess the presence of extracellular traps, release of PAD4, and citrullinated histones using light and confocal imaging. Figure 6A-ii shows extruded nuclear material outside a group of mononuclear cells, and the networks of extruded DNA (METosis) are associated with citrullinated histones and PAD4 as illustrated in 6A-iii, and 6A-iv respectively. These results suggest that PAD secretion by activated RA SF and RA tissue macrophages contributes to citrullination of extracellular antigens (native fibrinogen in this assay), and that METosis provides a mechanism for the release of intracellular citrullinated antigens including histones.

4. Discussion

SLOs and synovial ELSs are sites of autoAb production in autoimmune arthritis [5, 8, 27]. Herein we investigated the hypothesis that macrophages at these sites play a major role in protein citrullination and ACPA production. We demonstrated that in SLOs from CIA mice and ELSs from RA synovial biopsies macrophages express PAD4, co-localize with peptidyl citrulline and their activation results in PAD release and METosis. Furthermore, macrophage depletion in CIA decreases tissue citrulline and serum ACPA levels, whereas, presentation of peptidyl citrulline by FDCs to B cells induces T-cell dependent ACPA production.

The emergence of anti-CCP Abs prior to clinical manifestations is a hallmark of human and experimental autoimmune arthritis as confirmed in this study and reported earlier in CIA DBA/1 mice [22]. In RA, these autoAbs are detectable in the patients' sera >10 years before the onset of articular manifestations [28]; however, the mechanisms by which such systemic autoimmunity localizes to the affected joints, and the cells involved in this localization are still unknown. Nonetheless, in the context of the current accepted paradigm of RA evolution, the mucosal origin, macrophage activation and enhanced citrullination could contribute to disease pathogenesis and compartmentalization through multiple pathways. In the pre-clinical phase, environmental triggers such as cigarette smoke and microbial infections activate macrophages and other PAD-producing cells at the mucosal sites leading to extensive citrullination of intracellular and extracellular antigens. In the presence of defective tolerance and permissive genetic background, these citrullinated antigens are effectively presented leading to breach of tolerance and ACPA production [29, 30]. As the disease evolves, affinity maturation and epitope spreading promote humoral (ACPA) localization to the synovial tissues; meanwhile, inflammation-induced upregulation of homing receptors and addressins (e.g., α4β1/VCAM-1) on the mucosal immune cells and the synovium, respectively, mediates infiltration of the synovium with mononuclear cells [31, 32]. With further disease

progression, activated synovial tissue macrophages contribute to the local display of citrullinated intracellular and extracellular antigens during METosis and PAD release, respectively, thus promoting the final transition of systemic autoimmunity to the articular sites.

Activated macrophages can make up to 30–40% of the cellular content of the RA synovium [33], where several mechanisms can promote their activation and PAD-dependent citrullination. These mechanisms include (1) engagement of macrophage TLRs with microbial TLR ligands [34] including EBV that has been localized in RA synovia [35] and reported to trigger TLR activation of macrophages [36]; (2) Macrophage activation and complement fixation by ACPA immune complexes' binding FcgRs [37]; (3) Macrophages apoptosis [38] and bacterial-induced cytolysis [39] during which PADs are activated and released leading to presentation of intracellular and extracellular proteins [40].

While peripheral tissues like the mucosal surfaces have been widely studied as major sites of PAD production and antigen citrullination in RA [30], the CIA mouse model in this study challenges a role of the skin as a site of initial antigen entry in PAD4 expression and antigen citrullination. Interestingly, mycobacterium tuberculosis used in our antigen preparations with complete Freund's adjuvant has been reported to express arginine deiminase [41] which catabolizes free arginine into citrulline [42], however, to date, peptidyl arginine deiminases are only expressed in vertebrates with the only exception of *Porphyromonas gingivalis* [43] that citrullinates human fibrinogen and α-enolase [44].

In contrast to the skin, our data strongly supports an important role of resident lymphoid tissue macrophages in PAD4 expression, autoantigen citrullination and ACPA production. While, expression of PADs in SF and monocyte-derived macrophages has been reported and induction of antigen citrullination by macrophage activation using ionomycin has been studied [40], here we show that resident lymphoid tissue macrophages express and release

PAD4 in response to the more inflammation-related TLR4 ligand LPS, and that freshly aspirated SF macrophages and synovial organ cultures from RA patients spontaneously release PAD without further activation. The released enzyme was active and citrullinated arginine-containing peptides and native fibrinogen *in vitro* which implies that a similar role could be performed by macrophages *in vivo* leading to citrullination of extracellular antigens.

Our *in-situ* tissue analysis indicated that CD68+ve macrophages were largely co-distributed with PAD4 and peptidyl citrulline in the RA synovium, as calculated by Mander's correlation coefficient. However, due to the presence of PAD4 in the extracellular space where it cannot localize with the intracellular signal of CD68 and the expression of PAD4 by vessel-like structures in the synovium, the distribution was not completely overlapping. In fact, it was noticeable that, in the RA synovium, PAD4 has a branching serpentine labelling pattern, suggestive of vascular association, distinctive from the CD68 distribution. Although endothelial expression of PAD4 has been previously described [45], a smooth muscle cell or

→ other perivascular source cannot be excluded. Specifically, we selected CD68 as a pan-macrophage marker in order to explore PAD4 expression in all subsets of lymphoid tissue macrophages since other classic macrophage markers are lacking in certain subsets e.g. F4/80 in the subcapsular sinus macrophages, and CD11b in tangible body macrophages [46].

ELSs develop in the target tissues of rheumatic autoimmune diseases including the rheumatoid synovium [5, 8, 9, 27]. We have previously shown that B cells differentiated within synovial ELS in the RA joints frequently target deiminated proteins [17], and that fully functional ELSs with B cell proliferation, AID expression and ongoing CSR, produce human IgG ACPA in active GCs [7]. While the source of citrullinated antigens driving these local tissue reactions is still to be fully elucidated, our results show that CD68 macrophage express PAD4 and colocalize with peptidyl citrulline in the inflamed RA synovia and thus could be a major contributor to the local generation of citrullinated antigens which induces and maintains

synovial ACPA production. Although transport of citrullinated antigens from peripheral tissues cannot be excluded, several reports support that autoantigen citrullination is locally induced in the RA synovium. For example, citrullination of circulating extracellular antigens like fibrinogen and IgG has been reported to be dependent on local PAD expression [47]. Furthermore, *in vitro* treatment of RA synovial membranes with glucocorticoids reduced citrullinated proteins and PAD expression simultaneously [48]. Moreover, intracellular citrullinated proteins colocalize with PAD2 and correlate with local ACPA production in RA joints [49].

It is important to point out that whereas macrophages could contribute to the local generation of citrullinated antigens in RA SF and membranes, they are not the sole drivers of this process, and neutrophils can also release PADs which citrullinate extracellular antigens and provide citrullinated histones during NETosis [17, 50-52]. That said, macrophages uniquely mediate other functions beyond PAD expression and antigen citrullination; and it is the synergistic outcome of these functions that lend macrophages critical importance in anti-CCP production.

First, macrophages are professional APCs and we have shown their association with T cells in CIA SLOs and synovial ELSs. Remarkably, studies in mice have demonstrated that macrophages are the most important APC involved in processing and presentation of bovine collagen type II to T cells [53]. It was argued that the size and fibrillar nature of collagen type II influences antigen uptake and processing, and thus macrophages are the only type of APC able to present this antigen [54]. We reason that this might be also the case with other high molecular weight arthritogenic antigens including fibrinogen and extracellular matrix proteins. In addition, macrophages and T cells reciprocally activate each other in RA synovia. Macrophages TNF activated T cells, and T cell IFNγ enhances antigen presentation by macrophages [55-57]. With their capacity to citrullinate and present antigens to T cells,

macrophages could, thus, be a critical factor in breach of tolerance and autoimmunity in early
→ arthritis. Importantly, presentation of citrullinated antigens on appropriate MHC is essential for the development of anti-CCP antibodies . Actually, citrullination *per se* is inflammation-dependent and not RA specific [58], and in the absence of antigens that undergo citrullination and peptide presentation, as in pristane-induced arthritis, severe inflammatory arthritis develops without generation of anti-CCP Abs [59].

The critical role of citrulline-specific T cells in anti CCP production is supported by the results of our *in-vitro* GCRs which produced anti CCP IgG only in the presence of T cells. Although, we have previously shown that extensive crosslinking of BCRs by FDC-retained antigens may induce robust T cell independent IgM responses [24, 25], however, here we show that ACPA IgG production is T-cell dependent. We have also shown that FDC^+ ELSs invariably expressed AID and Iγ-Cμ circular transcripts indicating ongoing CSR in the rheumatoid synovium [7] supporting the role of ELSs in local production of this pathogenic Ig isotype. Indeed, it is the class-switched ACPA IgG isotype that is significantly associated
→ with the pre-clinical phase of RA [60] and with RA radiographic progression [61, 62]. It is plausible that the T cell help provided in the autoreactive GCs induced by citrullinated proteins and peptides is antigen specific. Antigen specificity of TFH cells in the GCs has been substantiated in immunized mice, where it has been reported that B cell – T cell contact during cognate recognition greatly amplifies the effective concentration of secreted cytokines across the immunological synapse [63], and that IL-4-producing T cells were found conjugated to GC B cells expressing high levels of AID, with evidence of somatic hypermutation [64]. In addition, prolonged contact between pMHCII-specific effector TFH cells and antigen-primed $pMHCII^+$ B cells at the T-B border in the pre-GC phase is a prerequisite for subsequent entry of effector TFH cells into the GC reaction [65].

Second, macrophages substantially contribute to ectopic lymphoid neogenesis where local autoAbs are generated. As lymphoid tissue inducers, the interaction between M1 macrophages and vascular smooth muscle cells has been proposed to contribute to the formation of ELSs in athrosclerosis in TNF/LT-dependent way [66-68]. In addition, as reports indicate that (1) FDCs emerge from perivascular precursors [69], (2) macrophages are major producers of TNF in active RA [70, 71], and (3) that TNF blockade kills macrophages and disrupts FDC reticula in RA synovia [72-74], it is highly plausible that macrophages contribute to FDC development in ELSs, thus, initiating sites of B cell recruitment, antigen-driven activation and auto-Ab production. Such contribution of macrophages to lymphoid neogenesis may explain the strong association of CD68 with the cellular components of ELS as shown by the analysis of RNA Seq data in our results.

Mobilization of intracellular citrullinated histones, a major target of ACPA Abs, to the extracellular space is mandatory for BCR-mediated B cell activation, plasma cell differentiation and Ab production. We have reported NETosis as a potential mechanism mediating this process → [17] , which has been recently linked to PAD4 expression and histone hypercitrullination [75]. Thus, we reason that a similar association exists for METosis. Indeed, here we show that LPS activation of macrophages (a cell lineage abundant in RA synovium) induces METosis contributing to citrullinated histones-driven autoimmunity.

The mechanisms of METosis in health and disease are unfolding [76, 77]. We anticipate that METosis contribution to citrullination and ACPA production extends beyond mobilization of intracellular citrullinated antigens to the extracellular space. For example, as a consequence of loss of the cell membrane, METosis leads to the release of PADs and intracellular Ca^{+2} from activated macrophages which provide optimum environment for extracellular antigen citrullination. Remarkably, macrophages in RA synovial membranes and fluids are chronically activated by several inflammatory stimuli which partly explains the extensive

METotic figures seen in freshly aspirated SF macrophages as well as resistance to further stimulation by LPS *in vitro*.

In conclusion, through comparable mechanisms of PAD release, extracellular antigen citrullination, and METosis [working model is schematically described in figure 7], our study shows the importance of macrophages in protein citrullination and ACPA production in SLOs and ELS contributing to systemic autoimmunity and articular localization of RA. Reducing citrullinated antigens, through selective targeting of macrophage PAD, may lead to the development of a novel therapeutic approach to induce long-term disease-free remission in RA.

Conflicts of interest

None.

Author contributions

ME: study design, experiments, data acquisition, data analysis, manuscript preparation and revision; **RE:** experiments, data acquisition, data analysis; **LFJ:** experiments, data acquisition, data analysis (animal data); **AN, RH:** experiments (clinical data); **KG, CR, ML:** RNA-Seq data acquisition and analysis ; **CP:** study design, interpretation of experimental results, manuscript preparation.

Funding

The research leading to these results has received funding from the Barts Charity grant number MRC0177. The Pathobiology of early arthritis cohort (PEAC) was funded by the MRC grant 36661. Additional funding from MRC funded - Maximising Therapeutic Utility for Rheumatoid Arthritis using genetic and genomic tissue responses to stratify medicines (MATURA) -Grant Ref: MR/K015346/1 and ARUK funded - Experimental Arthritis Treatment Centre (EATC) - Grant Ref: 20022. The animal work was supported by Arthritis Research UK Grants Reference 20305 & 20770.

Acknowledgments

We thank the core team members in the centre for Experimental Medicine and Rheumatology (EMR) – William Harvey Research Institute for retrieval and provision of the synovial tissue biopsies from the EMR BioBank.

Figure Legends

Figure 1: Expression of PAD4 in the secondary lymphoid tissues of CIA mice. Serum anti-CCP Ab levels **(A)** and arthritis scores **(B)** of CIA mice. WB of PAD4 in the draining LNs and skin at the site of antigen challenge **(C)** as well as spleens **(D)** from 3 different CIA mice. Recombinant PAD4 and GAPDH were used as positive and negative controls respectively. Confocal imaging of PAD4 (i, blue), CD11c (ii, green), and CD68 (iii, red) in CIA mice spleens **(E)** and draining LNs **(F)** sections are shown in three separate channels. The overlay of PAD4 and CD68 (iv), PAD4 and CD11c (v) and PAD4, CD68, and CD11c (vi) are shown. Scale bar 200 um. **(G)** Colocalization of PAD4 (blue) with medullary macrophages (CD68, red) in CIA LNs. Higher magnification is shown in the middle panel and the intracellular localization of PAD4 is shown in the lower panel. Scale bar 30 um. **(H)** Distribution of PAD4 (blue) in CIA LN cortex. The LN capsule is marked with *, the GCs are labelled with GL7 (green, GC B cells) and CR1/2 (red, FDCs) and marked with a white arrow; and the paracortex is indicated by **. Scale bar 100 um. **(I)** Colocalization of PAD4 (blue) with CD68 (red) TBMs in the GCs (green, GL7, GCBs). Single channels and overlays are shown. Scale bar 100 um. **(J)** High magnification of a TBM showing colocalization of CD68 (red), PAD4 (blue), and engulfed apoptotic GCB cell fragments (green). Scale bar 10 um. **(K)** WB of PAD4 in CD11b-purified macrophage lysates from the draining LNs and spleens of 3 different CIA mice. Controls as in C and D.

Figure 2: Distribution of citrullinated proteins / peptides in the draining LNs and spleens of CIA mice; and the impact of macrophage depletion on lymphoid tissue citrulline and serum ACPA levels. (A-i) IHC and confocal tile scanning of CD68 (red) and peptidyl citrulline (green) in a mid-saggital section of the draining LNs of CIA mice show cortical retention of peptidyl citrulline (white rectangle] and colocalization with CD68 in the medulla (dashed rectangle). Single colour channels are shown to the left of the merged image. High magnification imaging of

the LN medulla **(A-ii)** and cortex **(A-iii)** showing peptidyl citrulline distribution in relation to CD68. Scale bar 100 um. **(B-i)** IHC and confocal tile scanning of CD68 (red) and peptidyl citrulline (green) in CIA mice spleens showing peptidyl citrulline retention in follicular (white pulp – white ellipse) and extrafollicular (red pulp – dashed ellipse) regions. **(B-ii)** High magnification imaging shows colocalization of peptidyl citrulline with CD68 (**) and intrafollicular retention of peptidyl citrulline. Single color channels are shown to the left of the merged image. Scale bar 100 um. **(C, D)** DBA/1 mice were injected with F4/80 mAb i.p. for three successive days before injection of collagen II (CII) in CFA. Macrophage subsets were assessed by flow cytometry (dot plots in c) at day 0 (just before induction of CIA) and 3 weeks later and data is expressed as % of macrophages in total splenocytes (in D) **(E)** Citrulline content of the CIA spleens 3 and 4 weeks after CII/CFA administration with or without F4/80 treatment. Citrulline was measured by sandwich ELISA and expressed as ODs at 450 after normalization to the protein concentrations for each sample. **(F)** ELISA measurement of serum anti-CCP levels [weeks 1-4] in CIA mice with and without macrophage depletion using anti F4/80 mAb. Signifincance was calculated using unpaired 2-tailed student T test and the p values between F4/80 treated and untreated CIA (CII/CFA) mice are shown at the corresponding time point.

Figure 3: Activated murine macrophages release PAD4 and display extracellular trap formation (METosis). (A) Assessment of PAD activity in the culture supernatants of *in vitro* activated macrophages using different concentrations of LPS (10-1000 ng/ml). Conversion of peptidyl arginine into peptidyl citrulline by released PAD is detected in ELISA by specific mAb. PMA is included as a positive control. Signifincance was calculated using unpaired 2-tailed student T test and the p values between the unstimulated control and the treated conditions are shown. **(B)** Confocal imagining of purified splenic macrophages after 4 hr stimulation with 10ng/ml LPS. DNA is shown blue and DNA-associated citrullinated histones are shown in red. Unstimulated and PMA activated cells were used as negative and positive controls respectively.

High magnification of macrophage extracellular traps (METs) is shown on the right and citrullinated histones are indicated by white arrows. Scale bar = 50 μm except in the image with white arrows showing citrullinated histones, scale bar = 0.5 mm **(C)** Confocal imagining of in vitro generated TBM after 4 hr stimulation with 10ng/ml LPS. TBMs are labelled red (CD68), DNA (blue), and apoptotic B cells are labelled green with CSFE. Single channels, dual and triple colour overlays are shown and a high magnification of the released apoptotic B cell fragments in the METs are shown on the right (white arrow). Scale bare = 50 μm.

Figure 4: Induction of ACPA in in vitro GCRs and interaction of T and B cells with peptidyl citrulline-associated macrophages and FDCs in the draining LNs of CIA mice. **(A)** Low **(i)** and high **(ii, iii)** magnification confocal imaging of $CD3^+$ T cells (blue), $CD68^+$ macrophages (red) and peptidyl citrulline (green) in the draining LNs of CIA mice. The interaction between macrophages and T cells in the paracortex is represented in (iii, dashed ellipse). Scale bar 100 um. **(B)** Peptidyl citrulline (green) in the B cell follicles is retained on $CD21^+$ FDCs (red). Single colour channels are shown above the overlay. Scale bar 100 um **(C)** $ICOS^+$ Tfh cells (red) are seen in the light zone of the GC in association with peptidyl citrulline-retaining FDC reticula (blue) and PNA^+ activated GC B cells (green)in the draining LNs of CIA mice. Scale bar 100 um **(D)** GC in the DNLs of CIA mice labelled with anti-peptidyl citrulline (blue), the activated GC B cell marker (PNA, green), and the plasma cell marker Blimp 1 (red, white arrow). Scale bar 100 um. **(E)** Purified FDCs with dendritic morphology are shown with Nomarski optics (i), and the nuclei are stained blue (ii). Citrullinated fibrinogen (red) is shown on FDCs with rhodamine-conjugated anti fibrinogen Ab (iii) and few contaminating lymphocytes are shown adjacent to the white arrows. Scale bare = 10 μm. **(F)** Reconstitution of GCRs *in vitro* using citrullinated-fibrinogen IC-loaded FDCs with B and T cells from the spleens of CIA mice. The in vitro cultures are shown at day 1 (i) and day 5 (ii) after setup of the co-culture. **(G)** ACPA production in in vitro GCRs at day 5. Scale bar = 100 μm. Data expressed as the mean ± SEM.

Signifincance was calculated using 2-tailed unpaired student T test and the p value between FDC+T cell costimulated conditions and FDC-only co-culture controls is shown.

Figure 5: Expression of PAD4 and distribution of peptidyl citrulline in RA synovial tissues with ELSs. Low (i) and high (ii) magnification of IHC staining of RA synovial tissue macrophages (CD68, red) and PAD4 (green) in **(A);** and the distribution of peptidyl citrulline (blue) in relation to macrophages (CD68, green) in (**B**). **(C)** ELS stained for $CD20^+$ B cells (blue), macrophages (CD68, red) and PAD4 (green). Low and high magnifications are shown in (i) and (ii) respectively. **(D, E, and F)** low (i) and high (ii) magnification of adjacent RA synovial cryo-sections with ELSs (*). Colocalization of peptidyl citrulline (blue) with CD68 macrophages (red) and $CD3^+$ T cells (green) is shown in **D-i** with representative interaction between $CD3^+$ T cells and $CD68^+$ macrophages/peptidyl citrulline shown in **D-ii** (dashed ellipse). **(E-i)** Peptidyl citrulline (blue) retention on $CD21^+$ FDCs (green) indicated by white arrow in **E-ii** (corresponding to ELS with yellow*). **(F-i)** colocalization of peptidyl citrulline (blue), $CD20^+$ B cells (red) and $CD3^+$ T cells (green). **(F-ii)** High magnification of the ELS with yellow*. **(G-i)** Expression of the plasma cell-associated Blimp-1 transcription factor (red) in ELS of RA synovia with CD20+ B cells shown in green. **(G-ii)** High magnification of G-i with a white arrow pointing at Blimp-1. **(H)** Correlation of CD68 gene expression in RA synovia with various pathotypes and the histological scoring of T cells/CD3, B cells/CD20 and plasma cells/CD138. **(I)** Correlation of CD68 gene expression with CD3E (T cell-CD3e gene), CR2 (FDC-CD21 gene), MS4A1 (B cell-CD20 gene), and PRDM1 (plasma cell-Blimp-1 gene) in RA synovia. Correlation (r) and adjusted *p* values are shown with the corresponding plot. **(J)** *In situ* colocalization of CD68 (green), peptidyl citrulline (blue), and PAD4 (red) using Mander's correlation coefficient. Representative overlays of the probes are shown in i, ii, and iii; and the corresponding correlation plots are shown in iv, v, and vi respectively. In vii, a triple overlay of CD68, PAD4, and peptidyl citrulline shows intracellular [white box] extracellular [dashed white

box] and vessel-associated PAD4 [double white box] in the RA synovium. Scale bar 50 μm except Gii = 10 um

Figure 6: METosis and release of PAD from RA synovial fluid (SF) macrophages and organ cultures. (A-i) Enriched RA SF macrophages were cultured in vitro for 24 hrs in the presence or absence of different LPS concentrations (10-1000 ng/ml); and tonsillar macrophages were used as a control. PAD activity in the culture supernatants were assessed by ELISA and the ODs at 450 are shown. **(A-ii)** light microscopy of freshly aspirated RA SF macrophages show METosis (extruded network of nuclear material is marked with *). **(A-iii, iv)** Immunofluorescence of freshly aspirated RA SF showing METosis (networks of DNA, blue in iii and iv), release of citrullinated histones (red, white arrow in iii), and release of PAD4 (red, green → arrow in vi). (A-v) Anti citrullinated histone H3 shows no staining in SF macrophages from psoriatic arthritis patients (negative control) scale bar = 50 μm. **(B-i)** PAD activity in the culture supernatants and lysates of RA synovial membrane cultures. **(B-ii)** Schematic representation of the setup of synovial organ cultures, and an image of the actual cultures **(B-iii)** showing synovial tissue (S) on filter devices (F) cultured in medium (M). In A-i and B-i, signifincance was calculated using 2-tailed unpaired student T test and the p values between control tonsillar macrophages and synovial fluid macrophages and synovial organ culture supernatants are indicated.

Figure 7: Schematic representation of the proposed role lymphoid tissue macrophages in citrullination and ACPA production in autoimmune arthritis. Macrophage activation (1) by TLRLs, ICs, and proinflammatory cytokines induces PAD4 release which citrullinates native extracellular proteins (2), releases citrullinated intracellular antigens (e.g. citrullinated histones) by METosis (3); and presentation of citrullinated peptides to T cells (4). B cell activation by citrullinated antigens retained on FDCs (5) in the presence of T cell help (6) induces plasma cell differentiation and ACPA production.

Reference List

[1] J. U. Scher, S. B. Abramson. The microbiome and rheumatoid arthritis. NatRevRheumatol, 2011;7**:**569-78.

[2] K. D. Deane, C. I. O'Donnell, W. Hueber, D. S. Majka, A. A. Lazar, L. A. Derber *et al.* The number of elevated cytokines and chemokines in preclinical seropositive rheumatoid arthritis predicts time to diagnosis in an age-dependent manner. Arthritis Rheum, 2010;62**:**3161-72.

[3] J. A. Hamilton, P. P. Tak. The dynamics of macrophage lineage populations in inflammatory and autoimmune diseases. Arthritis Rheum, 2009;60**:**1210-21.

[4] Y. Imai, T. Sato, M. Yamakawa, T. Kasajima, A. Suda, Y. Watanabe. A morphological and immunohistochemical study of lymphoid germinal centers in synovial and lymph node tissues from rheumatoid arthritis patients with special reference to complement components and their receptors. Acta PatholJpn, 1989;39**:**127-34.

[5] A. Manzo, M. Bombardieri, F. Humby, C. Pitzalis. Secondary and ectopic lymphoid tissue responses in rheumatoid arthritis: from inflammation to autoimmunity and tissue damage/remodeling. ImmunolRev, 2010;233**:**267-85.

[6] L. Mandik-Nayak, B. T. Wipke, F. F. Shih, E. R. Unanue, P. M. Allen. Despite ubiquitous autoantigen expression, arthritogenic autoantibody response initiates in the local lymph node. ProcNatlAcadSciUSA, 2002;99**:**14368-73.

[7] F. Humby, M. Bombardieri, A. Manzo, S. Kelly, M. C. Blades, B. Kirkham *et al.* Ectopic lymphoid structures support ongoing production of class-switched autoantibodies in rheumatoid synovium. PLoSMed, 2009;6**:**e1.

[8] C. Pitzalis, G. W. Jones, M. Bombardieri, S. A. Jones. Ectopic lymphoid-like structures in infection, cancer and autoimmunity. NatRevImmunol, 2014;14**:**447-62.

[9] M. Bombardieri, M. Lewis, C. Pitzalis. Ectopic lymphoid neogenesis in rheumatic autoimmune diseases. NatRevRheumatol, 2017;13**:**141-54.

[10] S. Han, S. Cao, R. Bheekha-Escura, B. Zheng. Germinal center reaction in the joints of mice with collagen-induced arthritis: an animal model of lymphocyte activation and differentiation in arthritis joints. Arthritis Rheum, 2001;44**:**1438-43.

[11] C. Anzilotti, F. Pratesi, C. Tommasi, P. Migliorini. Peptidylarginine deiminase 4 and citrullination in health and disease. AutoimmunRev, 2010;9**:**158-60.

[12] C. Marchant, M. D. Smith, S. Proudman, D. R. Haynes, P. M. Bartold. Effect of Porphyromonas gingivalis on citrullination of proteins by macrophages in vitro. J Periodontol, 2013;84**:**1272-80.

[13] C. Foulquier, M. Sebbag, C. Clavel, S. Chapuy-Regaud, R. Al Badine, M. C. Mechin *et al.* Peptidyl arginine deiminase type 2 (PAD-2) and PAD-4 but not PAD-1, PAD-3, and PAD-6 are expressed in rheumatoid arthritis synovium in close association with tissue inflammation. Arthritis Rheum, 2007;56**:**3541-53.

[14] A. Suzuki, Y. Kochi, H. Shoda, Y. Seri, K. Fujio, T. Sawada *et al.* Decreased severity of experimental autoimmune arthritis in peptidylarginine deiminase type 4 knockout mice. BMCMusculoskeletDisord, 2016;17**:**205.

[15] V. C. Willis, N. K. Banda, K. N. Cordova, P. E. Chandra, W. H. Robinson, D. C. Cooper *et al.* Protein arginine deiminase 4 inhibition is sufficient for the amelioration of collagen-induced arthritis. ClinExp Immunol, 2017;188**:**263-74.

[16] S. Rosengren, N. Wei, K. C. Kalunian, N. J. Zvaifler, A. Kavanaugh, D. L. Boyle. Elevated autoantibody content in rheumatoid arthritis synovia with lymphoid aggregates and the effect of rituximab. Arthritis ResTher, 2008;10**:**R105.

[17] E. Corsiero, M. Bombardieri, E. Carlotti, F. Pratesi, W. Robinson, P. Migliorini *et al.* Single cell cloning and recombinant monoclonal antibodies generation from RA

synovial B cells reveal frequent targeting of citrullinated histones of NETs. AnnRheum Dis, 2016;75**:**1866-75.

[18] S. Kelly, F. Humby, A. Filer, N. Ng, M. Di Cicco, R. E. Hands *et al.* Ultrasound-guided synovial biopsy: a safe, well-tolerated and reliable technique for obtaining high-quality synovial tissue from both large and small joints in early arthritis patients. AnnRheum Dis, 2015;74**:**611-7.

[19] D. Aletaha, T. Neogi, A. J. Silman, J. Funovits, D. T. Felson, C. O. Bingham, III *et al.* 2010 rheumatoid arthritis classification criteria: an American College of Rheumatology/European League Against Rheumatism collaborative initiative. Ann Rheum Dis, 2010;69**:**1580-8.

[20] V. Krenn, L. Morawietz, G. R. Burmester, R. W. Kinne, U. Mueller-Ladner, B. Muller *et al.* Synovitis score: discrimination between chronic low-grade and high-grade synovitis. Histopathology, 2006;49**:**358-64.

[21] M. E. M. El Shikh, R. El Sayed, C. Pitzalis. Isolation and Characterization of Mouse and Human Follicular Dendritic Cells. Methods MolBiol, 2017;1623**:**113-23.

[22] K. A. Kuhn, L. Kulik, B. Tomooka, K. J. Braschler, W. P. Arend, W. H. Robinson *et al.* Antibodies against citrullinated proteins enhance tissue injury in experimental autoimmune arthritis. J Clin Invest, 2006;116**:**961-73.

[23] D. Hashimoto, A. Chow, C. Noizat, P. Teo, M. B. Beasley, M. Leboeuf *et al.* Tissue-resident macrophages self-maintain locally throughout adult life with minimal contribution from circulating monocytes. Immunity, 2013;38**:**792-804.

[24] M. E. El Shikh, R. M. El Sayed, A. K. Szakal, J. G. Tew. T-independent antibody responses to T-dependent antigens: a novel follicular dendritic cell-dependent activity. JImmunol, 2009;182**:**3482-91.

[25] M. E. El Shikh, R. M. El Sayed, S. Sukumar, A. K. Szakal, J. G. Tew. Activation of B cells by antigens on follicular dendritic cells. Trends Immunol, 2010;31**:**205-11.

[26] K. N. Cordova, V. C. Willis, K. Haskins, V. M. Holers. A citrullinated fibrinogen-specific T cell line enhances autoimmune arthritis in a mouse model of rheumatoid arthritis. The Journal of Immunology, 2013;190**:**1457-65.

[27] C. Pitzalis. Pathogenesis of rheumatoid arthritis: from systemic autoimmunity to localised joint disease. Drug DiscovToday, 2014;19**:**1152-4.

[28] M. M. Nielen, D. van Schaardenburg, H. W. Reesink, R. J. van de Stadt, I. E. van der Horst-Bruinsma, M. H. de Koning *et al.* Specific autoantibodies precede the symptoms of rheumatoid arthritis: a study of serial measurements in blood donors. Arthritis Rheum, 2004;50**:**380-6.

[29] K. D. Deane, V. M. Holers. The Natural History of Rheumatoid Arthritis. Clinical therapeutics, 2019.

[30] V. M. Holers, M. K. Demoruelle, K. A. Kuhn, J. H. Buckner, W. H. Robinson, Y. Okamoto *et al.* Rheumatoid arthritis and the mucosal origins hypothesis: protection turns to destruction. NatRevRheumatol, 2018;14**:**542-57.

[31] T. Garrood, L. Lee, C. Pitzalis. Molecular mechanisms of cell recruitment to inflammatory sites: general and tissue-specific pathways. Rheumatology (Oxford), 2006;45**:**250-60.

[32] M. Salmi, D. H. Adams, P. Trivedi, A. Hänninen, S. Jalkanen. Chapter 90 - Systemic Manifestations of Mucosal Diseases: Trafficking of Gut Immune Cells to Joint, Liver, and Pancreas. In: Mestecky J, Strober W, Russell MW, Kelsall BL, Cheroutre H, Lambrecht BN, editors. Mucosal Immunology (Fourth Edition), Boston: Academic Press; 2015, p. 1749-59.

[33] G. S. Firestein, N. J. Zvaifler. How important are T cells in chronic rheumatoid synovitis? Arthritis Rheum, 1990;33**:**768-73.

[34] Y. Zhao, B. Chen, S. Li, L. Yang, D. Zhu, Y. Wang *et al.* Detection and characterization of bacterial nucleic acids in culture-negative synovial tissue and fluid samples from rheumatoid arthritis or osteoarthritis patients. Sci Rep, 2018;8**:**14305.

[35] C. Croia, B. Serafini, M. Bombardieri, S. Kelly, F. Humby, M. Severa *et al.* Epstein-Barr virus persistence and infection of autoreactive plasma cells in synovial lymphoid structures in rheumatoid arthritis. AnnRheum Dis, 2013;72**:**1559-68.

[36] A. Farina, G. Peruzzi, V. Lacconi, S. Lenna, S. Quarta, E. Rosato *et al.* Epstein-Barr virus lytic infection promotes activation of Toll-like receptor 8 innate immune response in systemic sclerosis monocytes. Arthritis Res Ther, 2017;19**:**39.

[37] L. Laurent, C. Clavel, O. Lemaire, F. Anquetil, M. Cornillet, L. Zabraniecki *et al.* Fcgamma receptor profile of monocytes and macrophages from rheumatoid arthritis patients and their response to immune complexes formed with autoantibodies to citrullinated proteins. Ann Rheum Dis, 2011;70**:**1052-9.

[38] G. S. Firestein, M. Yeo, N. J. Zvaifler. Apoptosis in rheumatoid arthritis synovium. J Clin Invest, 1995;96**:**1631-8.

[39] V. M. Holers, N. K. Banda. Complement in the Initiation and Evolution of Rheumatoid Arthritis. Front Immunol, 2018;9**:**1057.

[40] E. R. Vossenaar, T. R. Radstake, H. A. van der, M. A. van Mansum, C. Dieteren, D. J. de Rooij *et al.* Expression and activity of citrullinating peptidylarginine deiminase enzymes in monocytes and macrophages. AnnRheum Dis, 2004;63**:**373-81.

[41] S. T. Cole, R. Brosch, J. Parkhill, T. Garnier, C. Churcher, D. Harris *et al.* Deciphering the biology of Mycobacterium tuberculosis from the complete genome sequence. Nature, 1998;393**:**537-44.

[42] M. Zuniga, G. Perez, F. Gonzalez-Candelas. Evolution of arginine deiminase (ADI) pathway genes. MolPhylogenetEvol, 2002;25**:**429-44.

[43] E. R. Vossenaar, A. J. Zendman, W. J. van Venrooij, G. J. Pruijn. PAD, a growing family of citrullinating enzymes: genes, features and involvement in disease. Bioessays, 2003;25**:**1106-18.

[44] N. Wegner, R. Wait, A. Sroka, S. Eick, K. A. Nguyen, K. Lundberg *et al.* Peptidylarginine deiminase from Porphyromonas gingivalis citrullinates human fibrinogen and alpha-enolase: implications for autoimmunity in rheumatoid arthritis. Arthritis Rheum, 2010;62**:**2662-72.

[45] X. Chang, R. Yamada, A. Suzuki, T. Sawada, S. Yoshino, S. Tokuhiro *et al.* Localization of peptidylarginine deiminase 4 (PADI4) and citrullinated protein in synovial tissue of rheumatoid arthritis. Rheumatology (Oxford), 2005;44**:**40-50.

[46] J. M. den Haan, L. Martinez-Pomares. Macrophage heterogeneity in lymphoid tissues. SeminImmunopathol, 2013;35**:**541-52.

[47] M. A. Badillo-Soto, M. Rodriguez-Rodriguez, M. E. Perez-Perez, L. Daza-Benitez, Y. G. J. J. Bollain, M. A. Carrillo-Jimenez *et al.* Potential protein targets of the peptidylarginine deiminase 2 and peptidylarginine deiminase 4 enzymes in rheumatoid synovial tissue and its possible meaning. EurJRheumatol, 2016;3**:**44-9.

[48] D. Makrygiannakis, S. Revu, M. Engstrom, K. E. af, A. P. Nicholas, G. J. Pruijn *et al.* Local administration of glucocorticoids decreases synovial citrullination in rheumatoid arthritis. Arthritis ResTher, 2012;14**:**R20.

[49] L. De Rycke, A. P. Nicholas, T. Cantaert, E. Kruithof, J. D. Echols, B. Vandekerckhove *et al.* Synovial intracellular citrullinated proteins colocalizing with peptidyl arginine deiminase as pathophysiologically relevant antigenic determinants of

rheumatoid arthritis-specific humoral autoimmunity. Arthritis Rheum, 2005;52**:**2323-30.

[50] J. Spengler, B. Lugonja, A. J. Ytterberg, R. A. Zubarev, A. J. Creese, M. J. Pearson *et al.* Release of Active Peptidyl Arginine Deiminases by Neutrophils Can Explain Production of Extracellular Citrullinated Autoantigens in Rheumatoid Arthritis Synovial Fluid. Arthritis Rheumatol, 2015;67**:**3135-45.

[51] Y. Zhou, B. Chen, N. Mittereder, R. Chaerkady, M. Strain, L. L. An *et al.* Spontaneous Secretion of the Citrullination Enzyme PAD2 and Cell Surface Exposure of PAD4 by Neutrophils. Front Immunol, 2017;8**:**1200.

[52] H. R. Hampton, T. Chtanova. The lymph node neutrophil. SeminImmunol, 2016;28**:**129-36.

[53] E. Michaelsson, M. Holmdahl, A. Engstrom, H. Burkhardt, A. Scheynius, R. Holmdahl. Macrophages, but not dendritic cells, present collagen to T cells. EurJImmunol, 1995;25**:**2234-41.

[54] B. Manoury-Schwartz, G. Chiocchia, C. Fournier. Processing and presentation of type II collagen, a fibrillar autoantigen, by H-2q antigen-presenting cells. EurJImmunol, 1995;25**:**3235-42.

[55] I. B. McInnes, B. P. Leung, R. D. Sturrock, M. Field, F. Y. Liew. Interleukin-15 mediates T cell-dependent regulation of tumor necrosis factor-alpha production in rheumatoid arthritis. NatMed, 1997;3**:**189-95.

[56] I. B. McInnes, G. Schett. Cytokines in the pathogenesis of rheumatoid arthritis. NatRevImmunol, 2007;7**:**429-42.

[57] E. A. James, M. Rieck, J. Pieper, J. A. Gebe, B. B. Yue, M. Tatum *et al.* Citrulline-specific Th1 cells are increased in rheumatoid arthritis and their frequency is influenced by disease duration and therapy. Arthritis Rheumatol, 2014;66**:**1712-22.

[58] E. R. Vossenaar, T. J. Smeets, M. C. Kraan, J. M. Raats, W. J. van Venrooij, P. P. Tak. The presence of citrullinated proteins is not specific for rheumatoid synovial tissue. Arthritis Rheum, 2004;50**:**3485-94.

[59] J. Tuncel, S. Haag, M. H. Hoffmann, A. C. Yau, M. Hultqvist, P. Olofsson *et al.* Animal Models of Rheumatoid Arthritis (I): Pristane-Induced Arthritis in the Rat. PLoS One, 2016;11**:**e0155936.

[60] H. Kokkonen, M. Mullazehi, E. Berglin, G. Hallmans, G. Wadell, J. Ronnelid *et al.* Antibodies of IgG, IgA and IgM isotypes against cyclic citrullinated peptide precede the development of rheumatoid arthritis. Arthritis ResTher, 2011;13**:**R13.

[61] E. Berglin, T. Johansson, U. Sundin, E. Jidell, G. Wadell, G. Hallmans *et al.* Radiological outcome in rheumatoid arthritis is predicted by presence of antibodies against cyclic citrullinated peptide before and at disease onset, and by IgA-RF at disease onset. Ann Rheum Dis, 2006;65**:**453-8.

[62] S. W. Syversen, P. I. Gaarder, G. L. Goll, S. Odegard, E. A. Haavardsholm, P. Mowinckel *et al.* High anti-cyclic citrullinated peptide levels and an algorithm of four variables predict radiographic progression in patients with rheumatoid arthritis: results from a 10-year longitudinal study. Ann Rheum Dis, 2008;67**:**212-7.

[63] M. Huse, B. F. Lillemeier, M. S. Kuhns, D. S. Chen, M. M. Davis. T cells use two directionally distinct pathways for cytokine secretion. Nat Immunol, 2006;7**:**247-55.

[64] R. L. Reinhardt, H. E. Liang, R. M. Locksley. Cytokine-secreting follicular T cells shape the antibody repertoire. Nat Immunol, 2009;10**:**385-93.

[65] T. Okada, M. J. Miller, I. Parker, M. F. Krummel, M. Neighbors, S. B. Hartley *et al.* Antigen-engaged B cells undergo chemotaxis toward the T zone and form motile conjugates with helper T cells. PLoS biology, 2005;3**:**e150.

[66] K. Guedj, J. Khallou-Laschet, M. Clement, M. Morvan, A. T. Gaston, G. Fornasa *et al.* M1 macrophages act as LTbetaR-independent lymphoid tissue inducer cells during atherosclerosis-related lymphoid neogenesis. CardiovascRes, 2014;101**:**434-43.

[67] R. Grabner, K. Lotzer, S. Dopping, M. Hildner, D. Radke, M. Beer *et al.* Lymphotoxin beta receptor signaling promotes tertiary lymphoid organogenesis in the aorta adventitia of aged ApoE-/- mice. The Journal of Experimental Medicine, 2009;206**:**233-48.

[68] K. Lotzer, S. Dopping, S. Connert, R. Grabner, R. Spanbroek, B. Lemser *et al.* Mouse aorta smooth muscle cells differentiate into lymphoid tissue organizer-like cells on combined tumor necrosis factor receptor-1/lymphotoxin beta-receptor NF-kappaB signaling. ArteriosclerThrombVascBiol, 2010;30**:**395-402.

[69] N. J. Krautler, V. Kana, J. Kranich, Y. Tian, D. Perera, D. Lemm *et al.* Follicular dendritic cells emerge from ubiquitous perivascular precursors. Cell, 2012;150**:**194-206.

[70] C. Q. Chu, M. Field, M. Feldmann, R. N. Maini. Localization of tumor necrosis factor alpha in synovial tissues and at the cartilage-pannus junction in patients with rheumatoid arthritis. Arthritis Rheum, 1991;34**:**1125-32.

[71] G. Dennis, Jr., C. T. Holweg, S. K. Kummerfeld, D. F. Choy, A. F. Setiadi, J. A. Hackney *et al.* Synovial phenotypes in rheumatoid arthritis correlate with response to biologic therapeutics. Arthritis ResTher, 2014;16**:**R90.

[72] Q. Q. Huang, R. Birkett, R. Doyle, B. Shi, E. L. Roberts, Q. Mao *et al.* The Role of Macrophages in the Response to TNF Inhibition in Experimental Arthritis. JImmunol, 2018;200**:**130-8.

[73] S. Onuora. Experimental arthritis: Anti-TNF kills the macrophage response. NatRevRheumatol, 2018;14**:**64.

[74] J. H. Anolik, R. Ravikumar, J. Barnard, T. Owen, A. Almudevar, E. C. Milner *et al.* Cutting edge: anti-tumor necrosis factor therapy in rheumatoid arthritis inhibits memory B lymphocytes via effects on lymphoid germinal centers and follicular dendritic cell networks. JImmunol, 2008;180**:**688-92.

[75] S. Mohanan, S. Horibata, J. L. McElwee, A. J. Dannenberg, S. A. Coonrod. Identification of macrophage extracellular trap-like structures in mammary gland adipose tissue: a preliminary study. Front Immunol, 2013;4**:**67.

[76] N. A. Aulik, K. M. Hellenbrand, C. J. Czuprynski. Mannheimia haemolytica and its leukotoxin cause macrophage extracellular trap formation by bovine macrophages. InfectImmun, 2012;80**:**1923-33.

[77] R. S. Doster, L. M. Rogers, J. A. Gaddy, D. M. Aronoff. Macrophage Extracellular Traps: A Scoping Review. JInnateImmun, 2018;10**:**3-13.

Table 1: List of Abs used in this study

Primary Abs:

Clone	Reactivity	Target	Host	Format	Vendor	Cat No.
N418	Mouse	CD11c	Ar. Hamster	AF 488	Biolegend	117311
FA-11	Mouse	CD68	Rat	AF 594	Biolegend	137020
145-2C11	Mouse	CD3e	Rat	Biotin	Biolegend	100304
GL7	Mouse	B and T cell activation antigen	Rat	FITC [IgM]	BD Biosciences	553666
7E9	Mouse	CD21/CD35 (CR1/CR2)	Rat	PE	Biolegend	123410
Polyclonal	Mouse / Human	Histone H3 (citrulline R2,R8,R17)	Rabbit	Un-conjugated	Abcam	ab5103
L26	Human	CD20 (cytoplasmic)	Mouse	Un-conjugated	Dako	M0755
F7.2.38	Human	CD3	Mouse	Un-conjugated	Dako	M7254
KP1	Human	CD68	Mouse	Un-conjugated	Dako	M0814
MI15	Human	CD138	Mouse	Un-conjugated	Dako	M7228
1F8	Human	CD21	Mouse	Un-conjugated	Dako	M0784
7E.17G9	Mouse	ICOS	Rat	PE	Biolegend	117405
Polyclonal	Human	CD3	Rabbit	Un-conjugated	Dako	A0452
F95	Mouse / Human	Peptidyl Citrulline	Mouse	Un-conjugated [IgM]	EMD Millipore	MABN328
Polyclonal	Mouse / Human	Blimp-1 (N-20)	Goat	PE	Santa Cruz Biotechnology	Sc-13203
B-Ly1	Human	CD20	Mouse	RPE	Dako	R7013
Polyclonal	Mouse / Human	PAD4	Rabbit	Un-conjugated	Abcam	ab50247

2ry Abs and other stains:

Polyclonal	Rabbit	IgG (H+L)	Donkey	F(ab')2 - AF 594	Jackson Immuno Research	711-586-152
Polyclonal	Rabbit	IgG (H+L)	Donkey	F(ab')2 - AF 647	Jackson Immuno Research	711-606-152
Polyclonal	Rabbit	IgG (H+L)	Donkey	F(ab')2 - AF 488	Jackson Immuno Research	711-546-152

Polyclonal	Mouse	IgM u chain	Donkey	F(ab')2 - AF 488	Jackson Immuno Research	715-546-020
Polyclonal	Mouse	IgM u chain	Goat	Dylight 649	Jackson Immuno Research	115-495-075
Polyclonal	Mouse	IgM u chain	Donkey	AF 594	Jackson Immuno Research	715-585-140
Polyclonal	Mouse	IgG (H+L)	Donkey	F(ab')2 - AF 647	Jackson Immuno Research	715-606-150
Polyclonal	Mouse	IgG (H+L)	Donkey	F(ab')2 - AF 488	Jackson Immuno Research	715-456-150
Polyclonal	Mouse	IgG (H+L)	Donkey	F(ab')2 - Rhodamine RX	Jackson Immuno Research	715-296-151
Peanut agglutinin (PNA)	Mouse	Galactose on GCB	Plant Lectin	Fluorescein	Vector Laboratories	FL1071
-	-	DNA	-	647 Nuclear Probe	ThermoFisher Scientific	R37106
-	-	Biotin	-	Streptavidin AF 647	Life Technologies	S32357

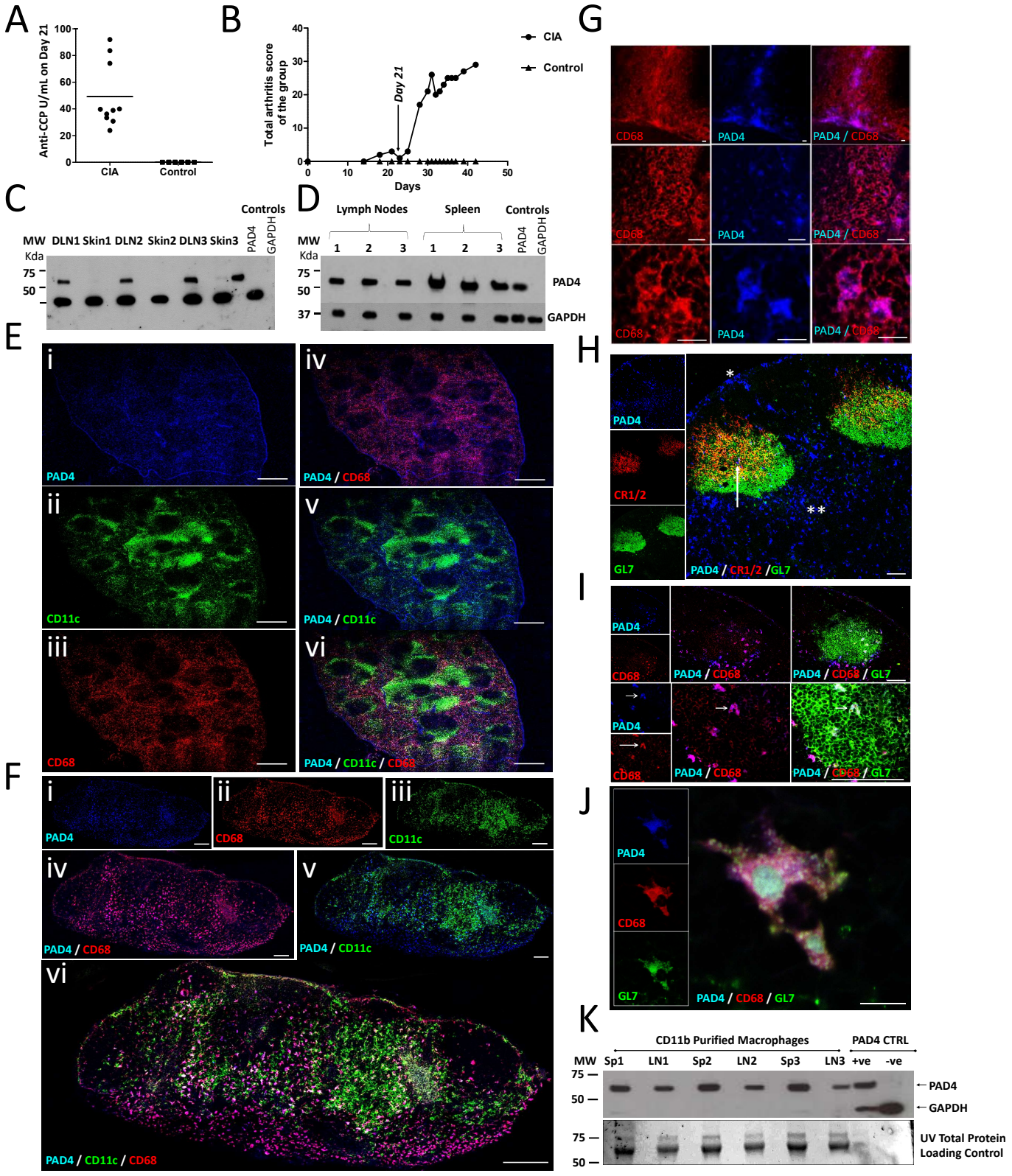
A
Anti-CCP U/mL on Day 21
CIA
Control
B
Total arthritis score of the group
Day 21
Days
CIA
Control
C
Controls
MW DLN1 Skin1 DLN2 Skin2 DLN3 Skin3
PAD4
GAPDH
Kda
75
50
D
Lymph Nodes
Spleen
Controls
MW
1 2 3 1 2 3
PAD4
GAPDH
Kda
75
50
37
E
i PAD4
ii CD11c
iii CD68
iv PAD4 / CD68
v PAD4 / CD11c
vi PAD4 / CD11c / CD68
F
i PAD4
ii CD68
iii CD11c
iv PAD4 / CD68
v PAD4 / CD11c
vi PAD4 / CD11c / CD68
G
CD68
PAD4
PAD4 / CD68
H
PAD4
CR1/2
GL7
PAD4 / CR1/2 /GL7
I
PAD4
CD68
PAD4 / CD68
PAD4 / CD68 / GL7
J
PAD4
CD68
GL7
PAD4 / CD68 / GL7
K
CD11b Purified Macrophages
PAD4 CTRL
MW Sp1 LN1 Sp2 LN2 Sp3 LN3 +ve -ve
75
50
PAD4
GAPDH
UV Total Protein Loading Control

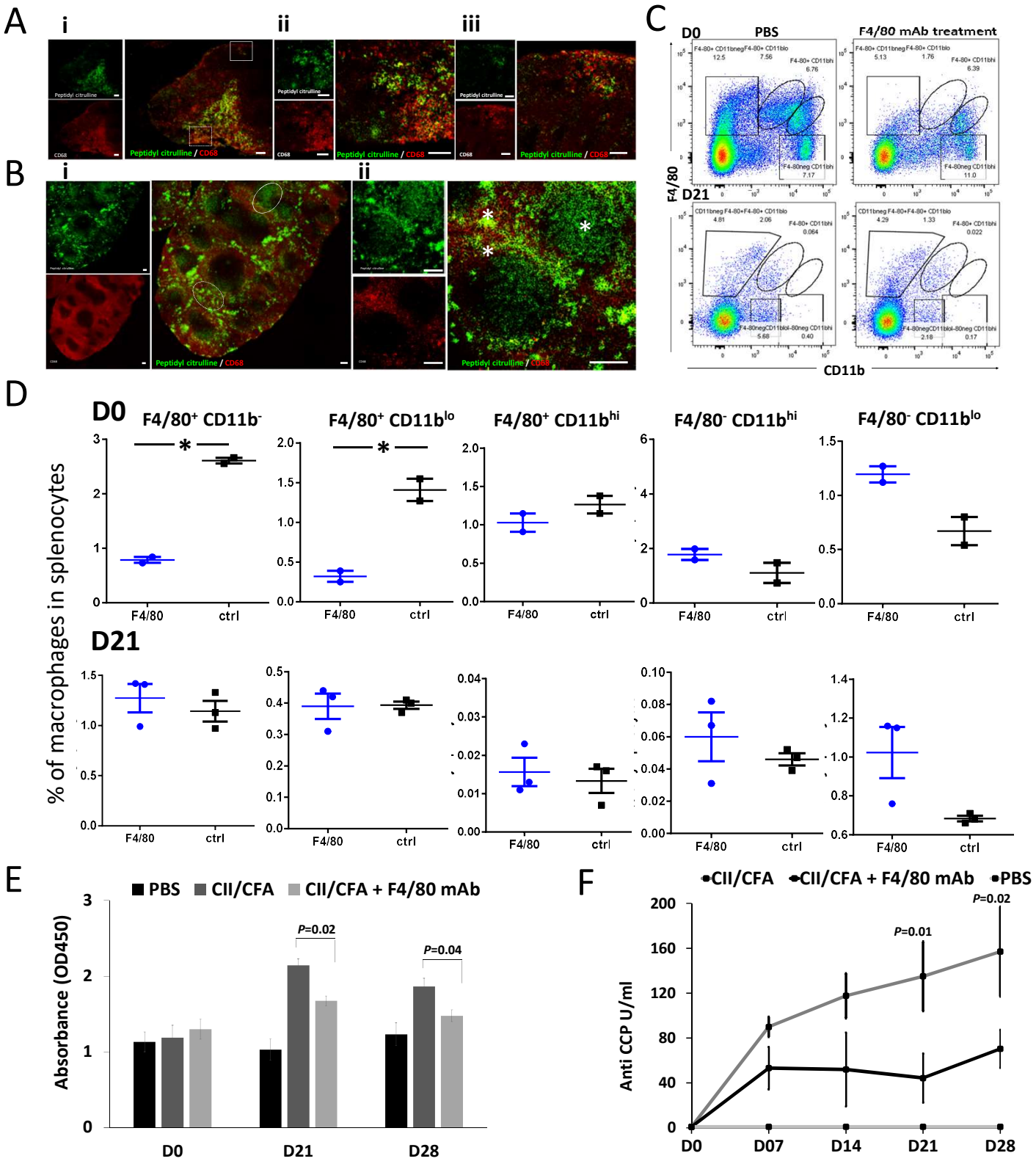
A
i
ii
iii
Peptidyl citrulline
CD68
Peptidyl citrulline / CD68
B
i
ii
C
D0
PBS
F4/80 mAb treatment
D21
F4/80
CD11b
D
D0
F4/80+ CD11b-
F4/80+ CD11blo
F4/80+ CD11bhi
F4/80- CD11bhi
F4/80- CD11blo
% of macrophages in splenocytes
F4/80
ctrl
D21
E
PBS
CII/CFA
CII/CFA + F4/80 mAb
Absorbance (OD450)
P=0.02
P=0.04
D0
D21
D28
F
CII/CFA
CII/CFA + F4/80 mAb
PBS
P=0.02
P=0.01
Anti CCP U/ml
D0
D07
D14
D21
D28

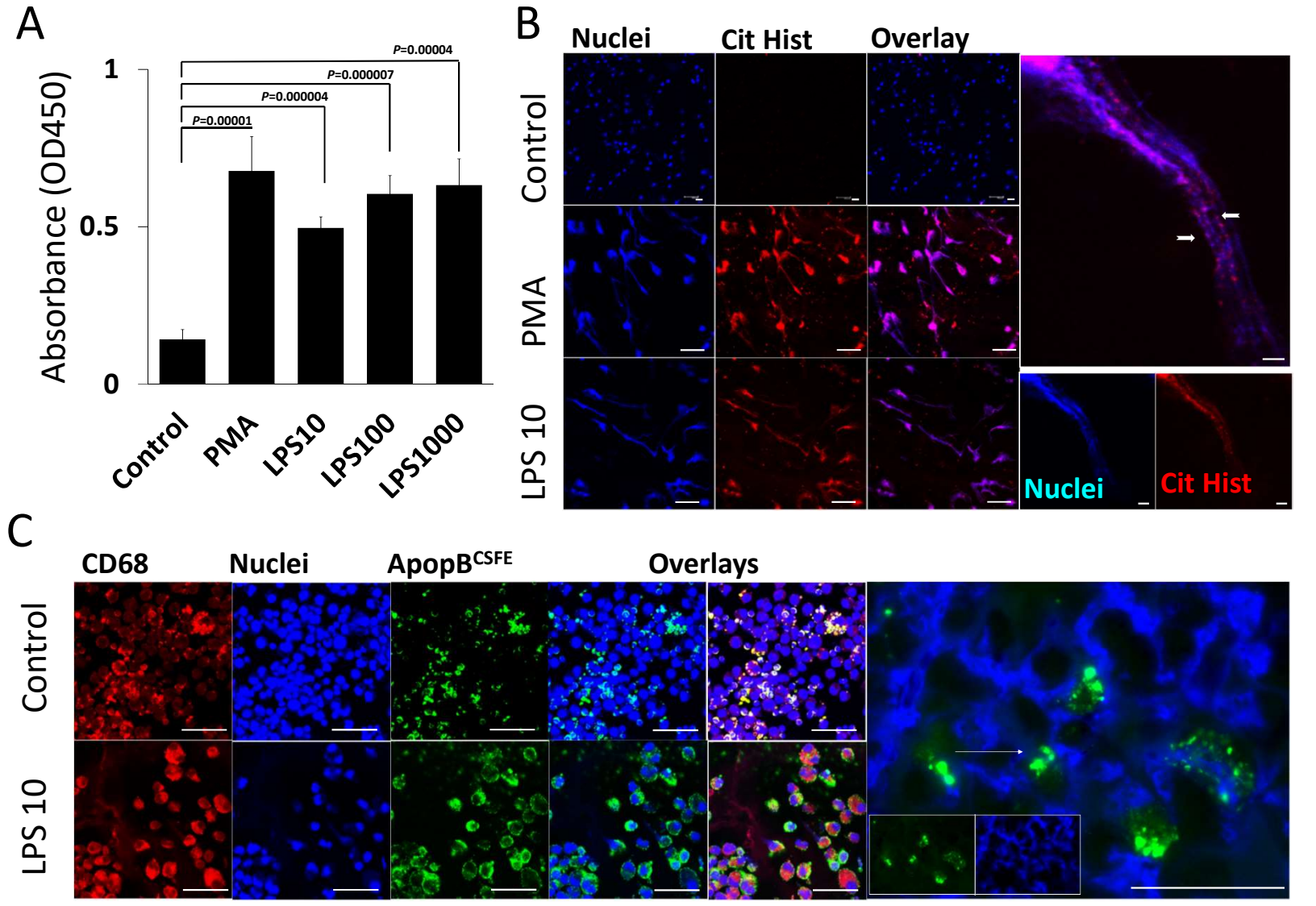
A
Absorbance (OD450)
1
0.5
0
P=0.00004
P=0.000007
P=0.000004
P=0.00001
Control
PMA
LPS10
LPS100
LPS1000
B
Nuclei
Cit Hist
Overlay
Control
PMA
LPS 10
Nuclei
Cit Hist
C
CD68
Nuclei
ApopB^CSFE
Overlays
Control
LPS 10

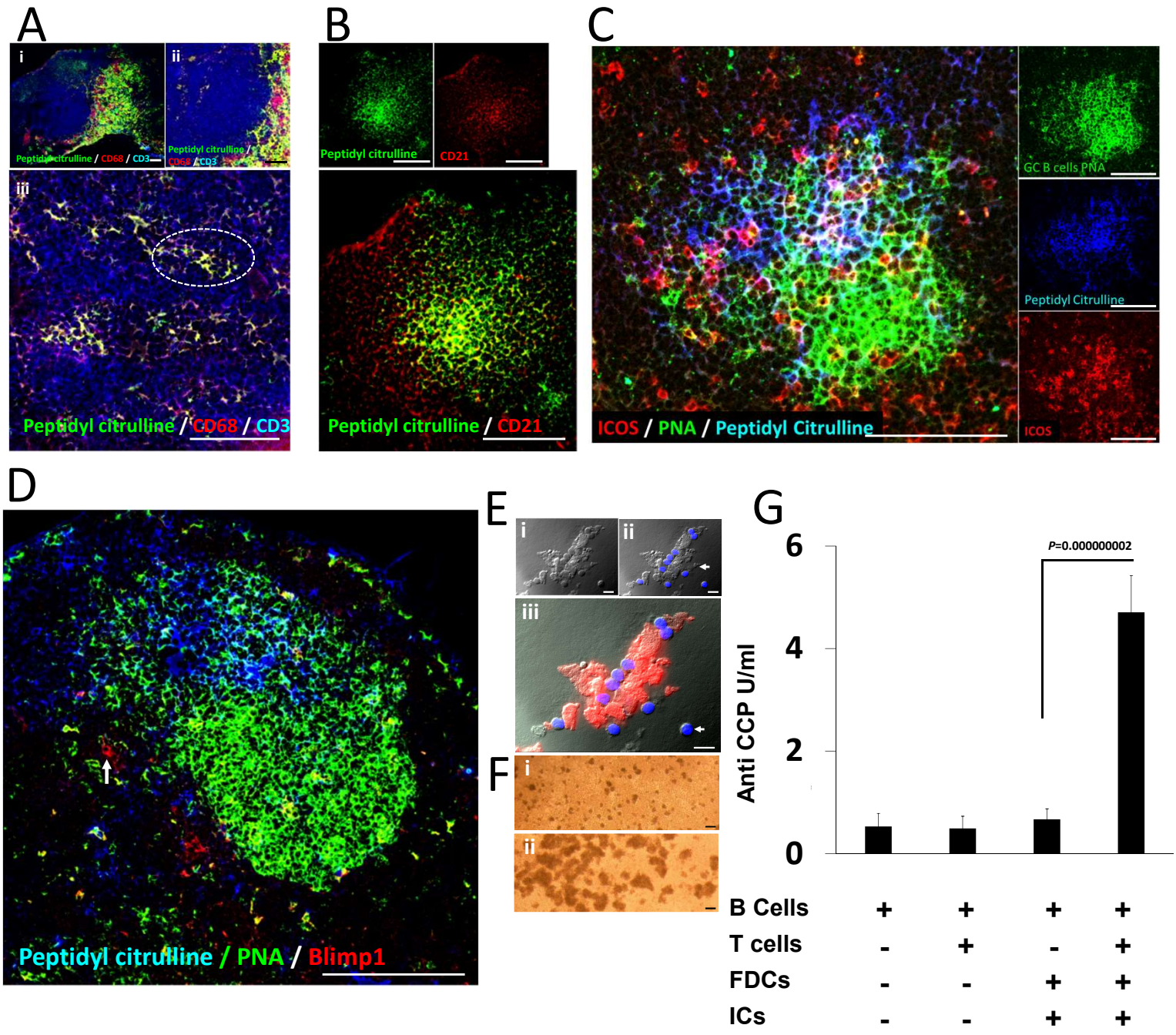
A
i
ii
iii
Peptidyl citrulline / CD68 / CD3
B
Peptidyl citrulline
CD21
Peptidyl citrulline / CD21
C
GC B cells PNA
Peptidyl Citrulline
ICOS
ICOS / PNA / Peptidyl Citrulline
D
Peptidyl citrulline / PNA / Blimp1
E
i
ii
iii
F
i
ii
G
Anti CCP U/ml
6
4
2
0
P=0.000000002
B Cells + + + +
T cells - + - +
FDCs - - + +
ICs - - + +

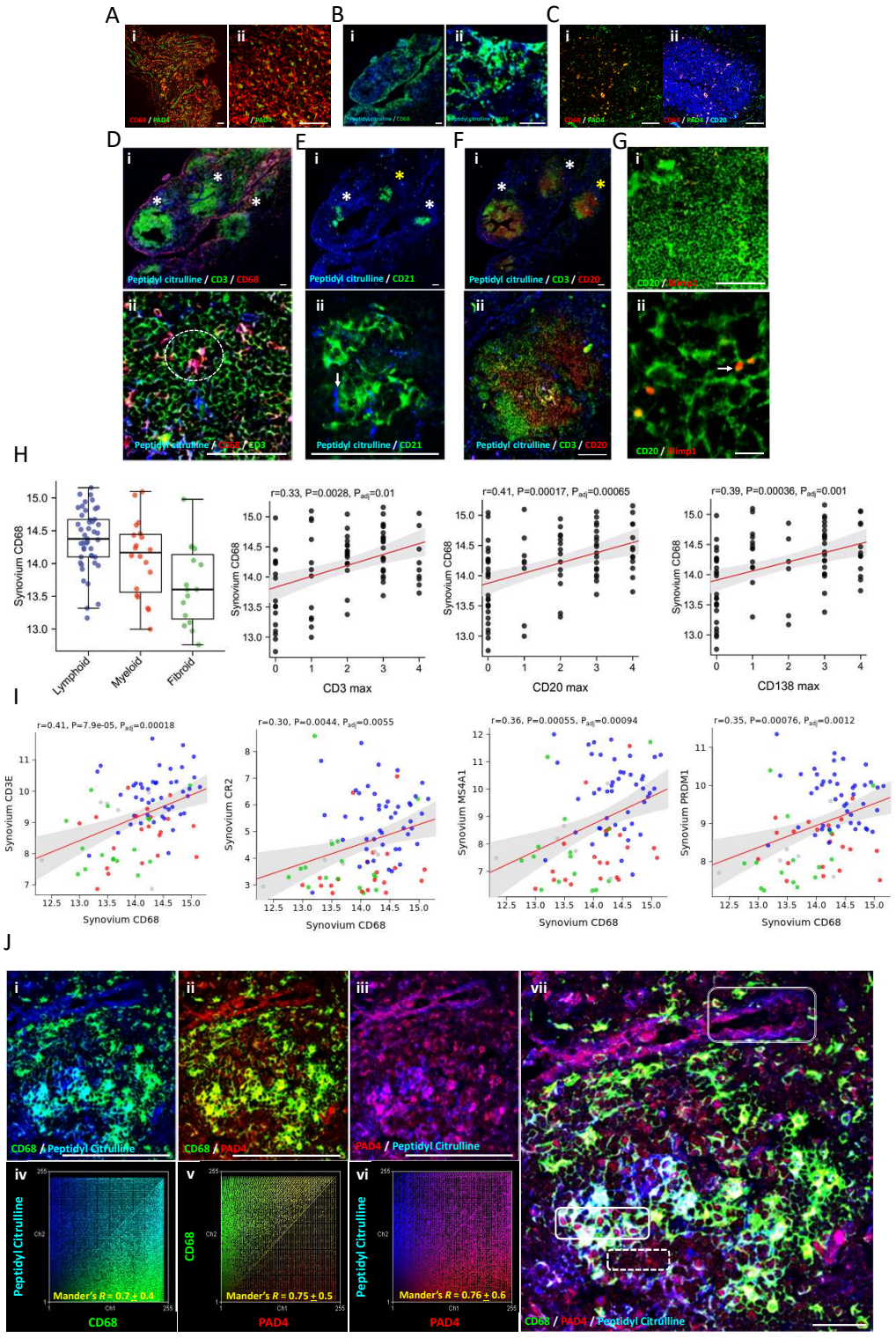
A
B
C
D
E
F
G
H
I
J
Peptidyl citrulline / CD3 / CD68
Peptidyl citrulline / CD21
Peptidyl citrulline / CD3 / CD20
CD20 / Blimp1
Synovium CD68
Lymphoid
Myeloid
Fibroid
r=0.33, P=0.0028, Padj=0.01
r=0.41, P=0.00017, Padj=0.00065
r=0.39, P=0.00036, Padj=0.001
CD3 max
CD20 max
CD138 max
r=0.41, P=7.9e-05, Padj=0.00018
r=0.30, P=0.0044, Padj=0.0055
r=0.36, P=0.00055, Padj=0.00094
r=0.35, P=0.00076, Padj=0.0012
Synovium CD3E
Synovium CR2
Synovium MS4A1
Synovium PRDM1
CD68 / Peptidyl Citrulline
CD68 / PAD4
PAD4 / Peptidyl Citrulline
Mander's R = 0.7 ± 0.4
Mander's R = 0.75 ± 0.5
Mander's R = 0.76 ± 0.6
CD68 / PAD4 / Peptidyl Citrulline

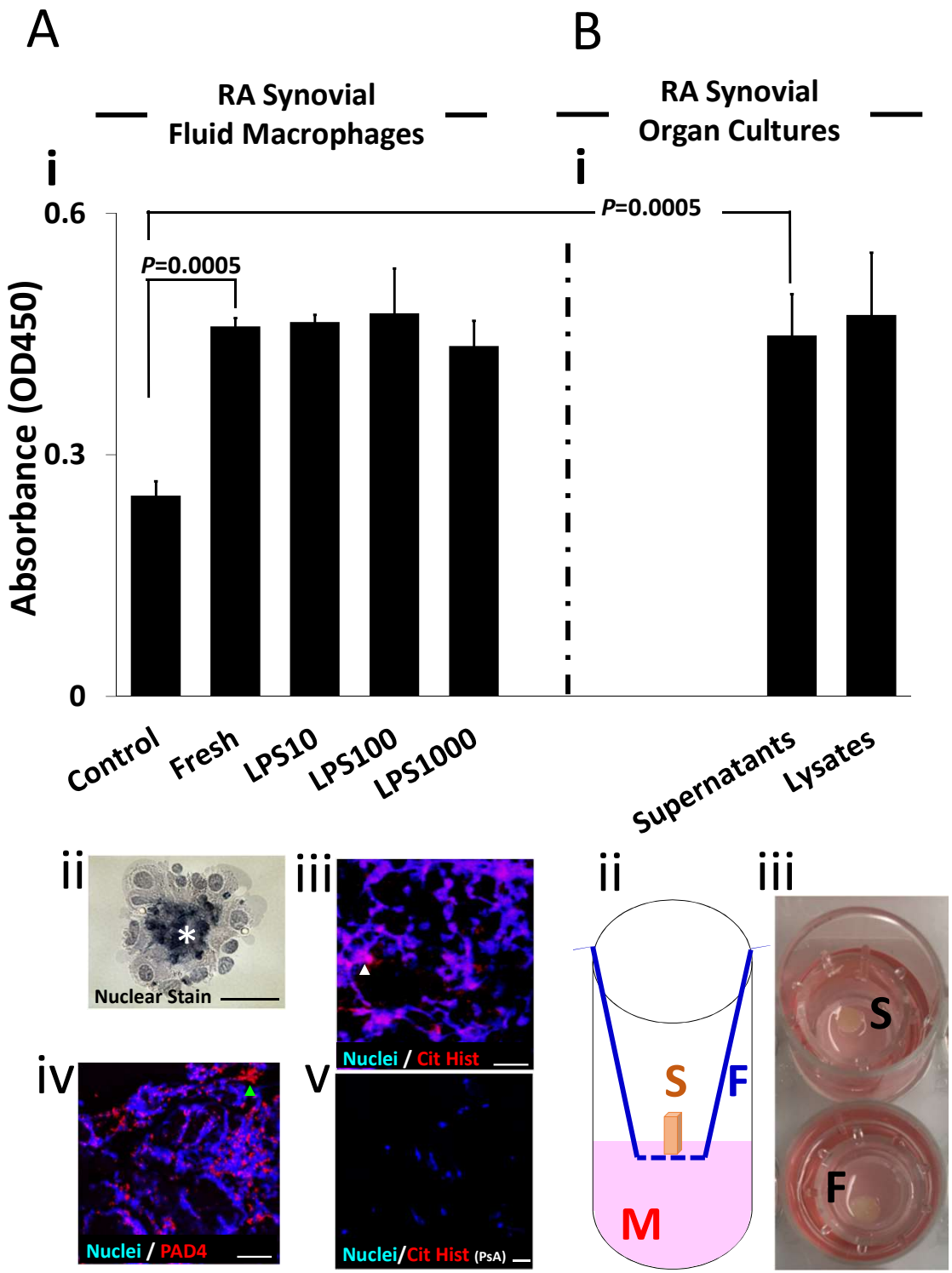
A
B
RA Synovial Fluid Macrophages
RA Synovial Organ Cultures
i
i
P=0.0005
P=0.0005
0.6
0.3
0
Absorbance (OD450)
Control
Fresh
LPS10
LPS100
LPS1000
Supernatants
Lysates
ii
iii
Nuclear Stain
Nuclei / Cit Hist
iv
v
Nuclei / PAD4
Nuclei/Cit Hist (PsA)
ii
iii
S
F
M
S
F

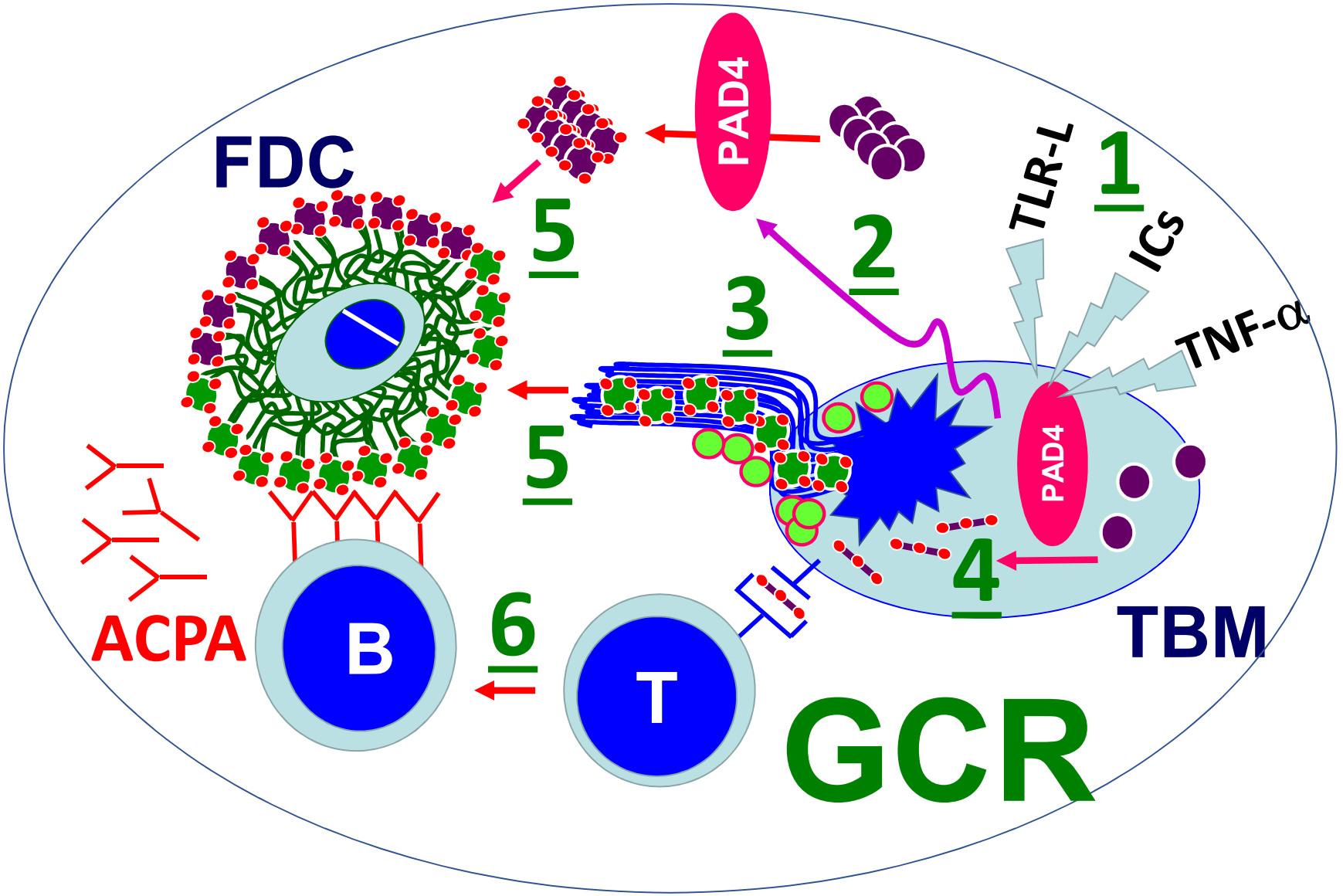
FDC
PAD4
TLR-L
ICs
TNF-α
1
2
3
4
5
5
6
PAD4
ACPA
B
T
TBM
GCR
Citrulline
Apoptotic cells (tingible bodies)
Citrullinated extracellular antigens
Citrullinated intracellular antigens
Citrullinated peptides
Native extracelluar antigens